http://dx.doi.org/10.1097/mm9.0000000000000028

MedMat

Review

OPEN

Organic Photoactive Materials with Aggregation-Induced Emission Characteristics for Tumor Theranostics

Chen Chen[a,b], Ping Wu[a], Feifan Zhao[a], Yuanyuan Han[a], Xiaoli Lu[a], Huan Yu[c], Lingyan Huang[c], Hao Wu[d,*], Xiaoying Chen[b,*] and Haijun Ma[a,*]

Abstract

Organic photoactive materials exhibit considerable potential in enhancing the precision of tumor diagnostics and therapeutics, owing to their distinctive photophysical characteristics and adaptable functional properties. Among these, aggregation-induced emission (AIE) materials exhibit superior performance attributes, including aggregation-enhanced fluorescence, robust photostability, and reduced background interference, thereby significantly enhancing the sensitivity of tumor imaging and therapeutic outcomes. This review focuses on the recent advancements in the design and application of AIE-based organic photoactive materials for tumor diagnostics and therapeutics. We elaborate on innovative design strategies centered on specific targeted subcellular organelle localization, tumor microenvironment-triggered activation, tunable emission wavelengths, and the integration of photoimmunotherapeutic functionalities. Moreover, this article presents a forward-looking perspective on the future development landscape of this field, emphasizing the critical role of organic photoactive materials in enhancing tumor theranostics. It also provides strategic guidance to facilitate the clinical translation of photodiagnostic approaches.

Keywords: Aggregation-induced emission, Malignant tumor, Organic photoactive materials, Phototheranostic

1. Introduction

Malignant tumors, characterized by high incidence and mortality rates, pose a significant challenge to global public health. The World Health Organization's latest statistics project over 20 million new cancer cases globally by 2025, with nearly 40% of these patients expected to face poor prognoses due to the constraints of current diagnostic and therapeutic technologies[1]. The conventional "gold standard" of tumor treatment, encompassing surgical resection, chemotherapy, and radiotherapy, encounters a trifold challenge in its practical application. Surgery often proves inadequate for eliminating subclinical metastatic lesions, and invasive procedures exacerbate the physiological stress of patients[2]. Chemotherapy induces considerable adverse effects and may precipitate drug resistance within the human body[3,4]. Radiotherapy-induced accidental injury to normal tissues has the potential to precipitate secondary neoplastic lesions[5]. These shortcomings highlight the urgent need for precise diagnostic techniques that achieve organic unity between "visualization and localization" and "minimally invasive treatment" at the molecular level.

The rise of phototheranostics has provided an innovative pathway to address the aforementioned challenges[6,7]. This strategy utilizes the photophysical properties of photoactive materials to synchronize optical imaging guidance and light-controlled therapeutic implementation using a single agent, thereby truly embodying the precision medicine concept of "what you see is what you treat"[8–10]. It has gained widespread recognition within the medical community. Theranostic agents, as the core elements of the phototheranostic process, directly determine its diagnostic and therapeutic efficiency. Among the various developed photoactive materials (such as inorganic quantum dots, upconversion materials, and fluorescent proteins)[11–14], aggregation-induced emission (AIE) materials have attracted significant attention due to their breakthrough "aggregation-enhanced luminescence" property[15–18]. In the aggregated state, the fluorescence intensity of AIE materials can be enhanced by 2 to 3 orders of magnitude. This unique behavior, characterized as "the more aggregated, the brighter they are," enables them to exhibit superior imaging signal-to-noise ratio and photostability in complex physiological environments. Furthermore, their excellent photostability and low photobleaching ensure stable fluorescence signal output under prolonged laser irradiation, providing technical

[a]*Key Lab of Ministry of Education for Protection and Utilization of Special Biological Resources in Western China, School of Life Sciences, Ningxia University, Yinchuan 750021, China,* [b]*State Key Laboratory of High-efficiency Utilization of Coal and Green Chemical Engineering, College of Chemistry and Chemical Engineering, Ningxia University, Yinchuan 750021, China,* [c]*General hospital of Ningxia medical university, Yinchuan 750004, China,* [d]*Max Planck Institute for Polymer Research, Ackermannweg 10, 55128 Mainz, Germany.*

**Corresponding authors: Address: Hao Wu, Max Planck Institute for Polymer Research, Ackermannweg 10, 55128 Mainz, Germany. E-mail address: wuh@mpip-mainz.mpg.de (H. Wu); Xiaoying Chen, State Key Laboratory of High-efficiency Utilization of Coal and Green Chemical Engineering, College of Chemistry and Chemical Engineering, Ningxia University, Yinchuan 750021, China. E-mail address: chenxiao18@nxu.edu.cn (X. Chen); Haijun Ma, Key Lab of Ministry of Education for Protection and Utilization of Special Biological Resources in Western China, School of Life Sciences, Ningxia University, Yinchuan 750021, China. E-mail address: mahj@nxu.edu.cn (H. Ma)*

MedMat (2026) 3:1

Received: 12 July 2025; Accepted 22 September 2025

Published online 29 September 2025

assurance for the long-term dynamic monitoring of tumor lesions[19,20]. Their high-brightness fluorescence also provides strong support for precise imaging. AIE materials can not only specifically target and enrich in tumor tissues through the enhanced permeation and retention effect, but their synergistic photothermal therapy (PTT) and photodynamic therapy (PDT) effects enable minimally invasive treatment of tumors. This offers innovative approaches to overcome the limitations of conventional therapies[21–23]. Crucially, the therapeutic efficacy of AIE-based photoactive materials exhibits a distinct aggregation-dependent activation characteristic. This intelligent, responsive mechanism significantly reduces nonspecific accumulation in normal tissues, effectively addressing the critical issue of systemic toxicity associated with traditional photosensitizers (PSs). It thereby provides an innovative solution for constructing integrated theranostic platforms[24].

While AIE materials hold great promise for in-tumor phototheranostics, their clinical implementation is hindered by several pivotal scientific challenges. First, the incomplete understanding of structure–activity relationships between material architectures and biological effects poses a significant obstacle to precise design. Second, the intrinsic compromise between tissue penetration depth and light energy conversion efficiency restricts the therapeutic effectiveness for deeply located tumors. Third, the lack of a comprehensive and multiscale system for evaluating biological effects hinders advancements in clinical translation[25]. This article provides a systematic review of recent progress in organic photoactive materials with AIE properties for cancer phototheranostics. It elucidates the intrinsic relationships among molecular design strategies, material properties, and biological effects, thereby highlighting key advancements and identifying prevailing challenges in the field. Moreover, it provides theoretical foundations for the development of next-generation precision tumor phototheranostic nanoplatforms, addressing fundamental challenges via meticulous material design and systematic biological assessment strategies.

2. Photoactive materials

In cancer phototheranostics, photoactive materials play a pivotal role, primarily encompassing photothermal conversion agents (PTCAs), PSs, and multifunctional nanoplatforms bearing photo-responsive moieties[26] (Figure 1). PTCAs represent a class of crucial reagents capable of efficiently capturing photon energy and converting it into thermal energy, thereby inducing cancer cell apoptosis through localized hyperthermia. PTCAs can be classified into 2 primary categories based on material types: organic and inorganic. Organic PTCA materials are predominantly composed of dye molecules with high absorption coefficients, such as indocyanine green (ICG), as well as nanoparticles (NPs) constructed from semiconductor polymers[27,28]. In contrast, inorganic PTCA materials encompass a diverse range of types, including noble metal nanostructures (e.g., gold NPs), transition metal chalcogenides and oxides (such as copper sulfide NPs), and carbon-based materials (e.g., graphene oxide)[29,30]. These materials have garnered attention due to their excellent optical performance and high photothermal conversion efficiency. On the other hand, PSs can be activated under illumination at specific wavelengths to generate singlet oxygen or other reactive oxygen species (ROS), thereby damaging cancer cells by inducing local oxidative stress. These materials are also classified into a series of high-performance organic dye molecules and a variety of inorganic materials, such as porphyrins and their derivatives and boron dipyrromethene (BODIPY)[31–33], as well as inorganic materials including titanium dioxide (TiO_2), zinc oxide, and graphitic carbon nitride, among others[34–36]. These PSs exhibit favorable light-absorbing properties in the visible or near-infrared (NIR) regions and are capable of efficiently generating ROS for cancer therapy. In summary, for different types of tumors and diverse therapeutic requirements, selecting appropriate photoactive materials is of paramount importance in enhancing the efficacy of cancer phototherapy. This article primarily elaborates on the research progress of organic photoactive materials in tumor diagnosis and therapy (Figure 1).

3. Tumor phototheranostics based on photoactive materials

3.1 The theranostic mechanisms of photoactive materials

Photoactive materials are pivotal in tumor treatment, particularly through PDT and PTT[37–39]. These modalities enable precise tumor ablation via distinct mechanisms, leveraging their noninvasive characteristics, high spatiotemporal selectivity, and minimal systemic toxicity[40]. Consequently, they have become central focuses in contemporary research.

The core mechanism of PDT hinges on the photochemical reactions of PSs when activated by light at specific wavelengths. These PS are typically organic molecules with conjugated structures (e.g., porphyrins, phthalocyanines) or inorganic nanomaterials (e.g., titanium dioxide [TiO_2])[41–43]. Upon absorbing photons at designated wavelengths (visible or NIR), the PS undergoes an electronic transition from its ground state (singlet) to an excited triplet state. This excitation triggers the generation of ROS through 2 primary pathways (Figure 2)[44]. Type I reaction involves the PS transferring electrons to the surrounding substrate (e.g., water or biomolecules), resulting in the generation of free radicals such as superoxide anion ($\cdot O_2^-$) and hydroxyl radical ($\cdot OH$)[45]. Type II reactions involve the PS directly transferring energy to ground state oxygen ($^3O_2$), thereby producing highly toxic singlet oxygen ($^1O_2$), which constitutes the primary ROS responsible for cell death in PDT[46]. The ROS induce tumor cell apoptosis or necrosis by oxidizing and damaging critical cellular structures, including cell membranes, mitochondria, and DNA. The advantage of PDT lies in its dual selectivity: PSs preferentially accumulate in tumor tissues, while light irradiation is localized to the targeted lesions, thereby minimizing damage to healthy tissues[47,48]. The therapeutic potential of PDT is hindered by 2 primary factors: the shallow tissue penetration of traditional visible light and the oxygen-deprived tumor milieu, which impedes ROS production due to its dependency on oxygen. To overcome these limitations, research has increasingly focused on developing NIR-activated PSs and integrating them with oxygen-carrying agents, representing a potent strategy for enhancing PDT outcomes[49–51]. PTT is a treatment modality based on the conversion of photon energy into thermal energy. This process involves the utilization of photoactive materials that absorb light at specific wavelengths, typically in the NIR range, and convert it into heat. This localized hyperthermia effectively induces thermal ablation of cancer cells at tumor sites[27,52]. Given its strong tissue penetration and minimal tissue absorption, NIR light has become the predominant light source for PTT applications[53].

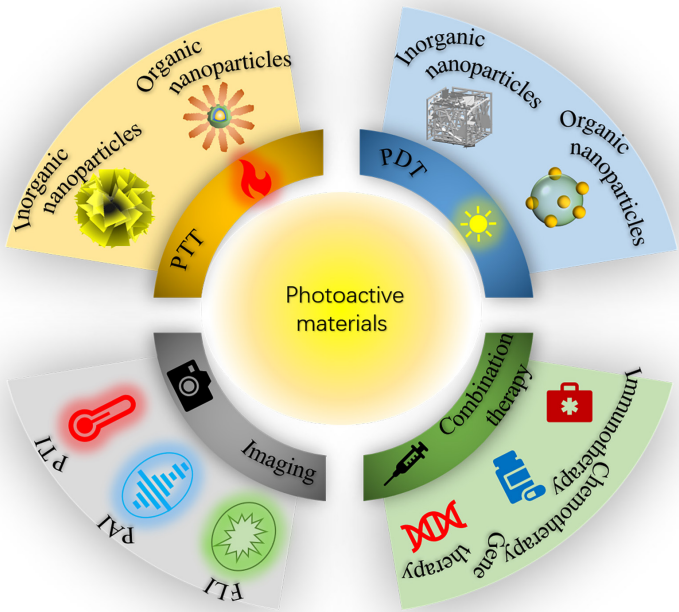

Figure 1. Schematic illustration of the application of photoactive materials in cancer therapy. FLI, fluorescence imaging; PAI, photoacoustic imaging; PTI, photothermal imaging.

Within biomedical imaging, multimodal approaches leveraging photoactive materials exhibit augmented diagnostic and therapeutic potentials via disparate signal transduction pathways[54,55]. Fluorescence imaging, a cornerstone optical modality, capitalizes on distinctive emissions from PSs like porphyrin derivatives or fluorescent NPs such as quantum dots and upconverting NPs doped with rare earth elements. These agents, when excited at precise wavelengths, facilitate intraoperative tumor delineation in real time. Nonetheless, the clinical implementation of this approach is impeded by tissue autofluorescence interference[54,56]. This challenge can be alleviated via the refinement of time-resolved fluorescence methodologies[57,58]. PAI, as another crucial imaging technology, innovatively combines optical contrast with the deep penetration capabilities of ultrasound. By leveraging the thermoelastic expansion effect induced by the absorption of pulsed laser light in photoactive materials, PAI facilitates real-time temperature field monitoring during PTT. This capability stems from the temperature dependence of the Grüneisen parameter (Γ), a key physical quantity governing the efficiency of converting absorbed optical energy into acoustic waves ($\Gamma = \beta c^2/C_p$, where β is the thermal expansion coefficient, c is the speed of sound, and C_p is the specific heat capacity). As temperature increases within the photothermal ablation zone, the local Γ value changes, leading to measurable variations in the generated photoacoustic signal amplitude. These variations provide quantitative insights into the dynamic regulation of thermal ablation zones[59–61]. In contrast, PTI captures the local temperature gradient distribution arising from the photothermal conversion in materials using an infrared focal plane array detector. This technique offers merits such as noninvasiveness, rapidity, and contactless temperature measurement. Despite its limited imaging specificity due to heterogeneous thermal conductivity between tumor microenvironments (TMEs) and normal tissues, it remains valuable for assessing hyperthermia response and therapeutic efficacy[62,63].

The trimodal fusion imaging system generates significant synergistic effects through complementary signal dimensions: (1) spatiotemporal resolution complementarity: fluorescence imaging provides molecular dynamic information, PAI resolves deep anatomical structures, and PTI captures metabolic thermodynamic characteristics[64–66]; (2) structural–functional complementarity: fluorescent markers target tumor-specific biomarkers, photoacoustic signals delineate vascular network topology, and photothermal signals reflect tissue metabolic activity[67]; (3) theranostic synergy refers to the integration of therapeutic and imaging mechanisms, characterized by multimodal energy conversion and functional complementarity[68]. For instance, NIR light can not only drive PTT to generate thermal energy but also excite PAI to produce ultrasonic signals, enabling simultaneous therapy and imaging[69]. PSs simultaneously facilitate ROS generation and tumor targeting, thereby enhancing the precision of theranostic applications[70]. Notably, these modalities differ significantly in spatiotemporal selectivity, excitation light requirements, and adaptability to the microenvironment. Specifically, PDT reliance on oxygen enables the use of imaging to assess tumor hypoxia, informing treatment strategies. Conversely, the thermal diffusion limitations inherent in PTT can be dynamically managed using PTI, allowing for optimized light dosage adjustments. Current research is focused on developing multifunctional nanoplatforms that integrate NIR responsiveness, oxygen self-supply, and pH sensitivity to overcome the limitations of individual techniques and advance "visualized therapy" and personalized theranostics.

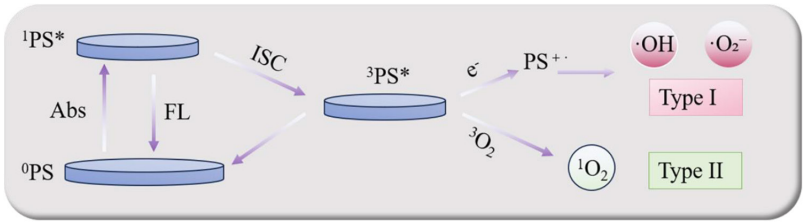

Figure 2. Types of ROS generation. ISC, intersystem crossing.

3.2 Innovative design of photoactive materials

In recent years, with the continuous deepening of the interdisciplinary integration between nanotechnology and biomedicine, the application of photoactive materials in the field of cancer therapy has garnered increasing attention. Researchers are increasingly exploring targeted approaches and synergistic therapeutic strategies to augment the specificity of these materials in eradicating cancer cells while mitigating collateral harm to healthy tissues[71,72]. Targeted drug delivery is facilitated through meticulous design and surface modification of nanomaterials, enabling their selective recognition and binding to tumor cell receptors. Consequently, this approach markedly enhances therapeutic effectiveness while concurrently mitigating the prevalent adverse effects linked to conventional chemotherapy[73]. Furthermore, exploiting the distinct physicochemical properties of the TME, including hypoxia, acidic pH, high redox state, etc, researchers have leveraged these features to develop a series of intelligent photoactive materials[74,75]. These materials are capable of undergoing physical or chemical changes upon exposure to specific external light sources, releasing reactive substances or heat to directly disrupt the structure of cancer cells, or activating immune response to indirectly eliminate tumor cells. Notably, the integration of multiple therapeutic modalities (such as the combination of PTT, PDT with chemotherapy or immunotherapy) can be achieved, overcoming the limitations of single-modal therapies and providing cancer patients with safer and more effective treatment regimens[76].

3.2.1 Subcellular organelle-specific targeted photoactive materials

As the critical challenges associated with the TME, such as heterogeneity, hypoxia, and immunosuppression, become increasingly prominent, the therapeutic strategies involving photoactive materials are undergoing a profound transformation from single-target breakthroughs to multisystemic regulation[77–79]. By precisely localizing the substructures of tumor cells, researchers are integrating photothermal/photodynamic effects with the activation of cell death pathways, thereby gradually establishing a spatiotemporally synergistic precision therapy framework[80]. This evolutionary process encompasses not only the expansion of targeting dimensions (from single-targeting to dual-targeting) but also the in-depth refinement of single-targeting systems, ultimately propelling tumor therapy from localized interventions to the regulation of metabolic networks[81].

The therapeutic strategies involving photoactive materials for tumor treatment have undergone significant advancements, transitioning from single-target breakthroughs to multisystemic regulation. Early single-targeting research primarily focused on the precise localization of subcellular structures. The TCF series of AIE PS developed by the Gong Ping group (Figure 3A), designed to target specific organelles such as mitochondria, the ER, and lipid droplets[82]. The multifaceted effects of a single target were revealed through TCF-Mem, which targets the cell membrane. Upon photoactivation, TCF-Mem induces pyroptosis and releases damage-associated molecular patterns (DAMPs) and inflammatory cytokines. This approach couples local treatment with systemic immune modulation for the first time. This discovery not only confirmed the efficacy of single-target approaches but also underscored the complexities introduced by tumor metabolic compensatory mechanisms. Specifically, TCF-Mito, which targets mitochondria and disrupts energy metabolism, may inadvertently facilitate cancer cell survival via lysosomal autophagy pathways. It provides a critical impetus for the development of dual-targeting synergistic strategies. Building upon the elucidation of single-targeting mechanisms, researchers have observed that the metabolic compensation effects in tumor cells frequently lead to the failure of single-target therapies. Consequently, they have embarked on exploring spatiotemporally precise dual-targeting designs to impede cellular escape pathways. This endeavor has propelled the rapid development of dual-targeting strategies, the crux of which lies in synergistic spatial localization and temporal effect superposition to block cellular escape routes[86–89]. Zhuang et al.[83] developed an aggregation-induced NIR-II emissive PS, DPITQ, via molecular engineering. Its lipophilic and cationic nature aligns with cancer cell physiology, featuring high lactate anion expression and hyperpolarized mitochondrial membrane potential (MMP), enabling selective accumulation at both plasma membranes and mitochondria (Figure 3B). This dual-targeting design facilitates spatiotemporally precise activation of type I/II ROS pathways under illumination, concurrently inducing pyroptosis and apoptosis to block tumor cell escape. DPITQ NPs achieve a high photothermal conversion efficiency of 57% while maintaining excellent metabolic stability, resulting in superior phototherapeutic outcomes.

The spatial confinement–mechanistic synergy design philosophy has been further extended and innovated in the microneedle patch system developed by Liu et al.[90] An intelligent combination of mitochondria-targeting AIE molecules and lysosome-targeting aluminum phthalocyanine (AIE-mito-TPP/AlPcSNa$_4$@MN) achieves a 99% inhibition rate in melanoma models by disrupting energy metabolism (ATP synthesis) and degradation systems (lysosomal membrane permeabilization). This dual-targeting strategy efficiently kills tumor cells at low doses (6 μg) by synergistically disrupting energy metabolism and degradation systems. Furthermore, the PPRK@MTO nanomedicine developed by Liang et al.[84] achieves highly efficient synergistic therapy through precise dual-organelle targeting (Figure 3C). This system utilizes an ER-targeting peptide, PPRK, to guide the specific accumulation of the nanomedicine in the tumor cell ER, enhancing the ROS generation efficiency of PDT by 3.1-fold. Simultaneously, the mitochondrial-targeting component, MTO, selectively inhibits the mitochondrial calcium uniporter (MCU)

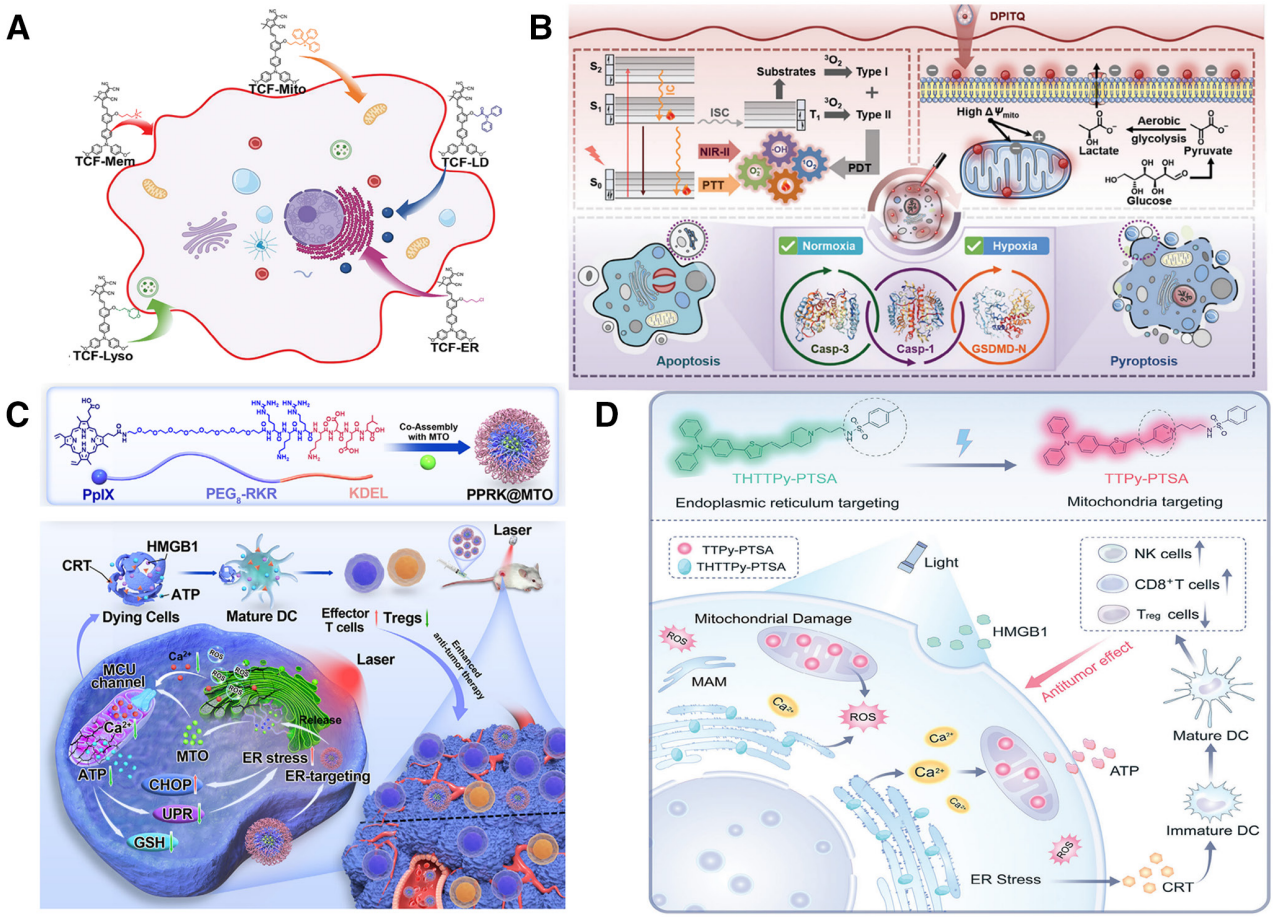

Figure 3. (A) Schematic illustration of the specific targeting of different organelles by TCF series photosensitizers[82]. Copyright 2024, Wiley-VCH Verlag GmbH & Co. KGaA, Weinheim. (B) Diagram depicting the mechanism of action of DPITQ[83]. Copyright 2023, Wiley-VCH Verlag GmbH & Co. KGaA, Weinheim. (C) Schematic representation of the preparation and mechanism of action of PPRK@MTO[84]. Copyright 2025, Wiley-VCH Verlag GmbH & Co. KGaA, Weinheim. (D) Schematic diagram showing THTTPy-PTSA modulating ER stress-mitochondrial damage for cancer immunotherapy[85]. Copyright 2024, Wiley-VCH Verlag GmbH & Co. KGaA, Weinheim.

channel, blocking calcium influx and disrupting mitochondrial–ER metabolic coupling. This spatially precise regulation results in a 2.3-fold increase in the expression of the ER stress marker GRP78, causing the collapse of the unfolded protein response by inhibiting ATP/GSH synthesis, and ultimately enhancing dendritic cell (DC) maturation by 50.7%. In the 4T1 breast cancer model, a single administration achieves an 85.28% tumor inhibition rate, underscoring the unique advantages of dual-subcellular organelle targeting strategies. These breakthroughs underscore that dual-targeting strategies can generate a "spatiotemporal resonanc" synergistic effect by intervening at key nodes of the metabolic network. However, their complexity has also spurred the in-depth refinement of single-targeting systems.

Notably, the advancement in dual-targeting research has inversely propelled the intelligent upgrading of single-targeting technologies. The BTZPP NPs developed by Huang et al.[91] have elevated lysosomal targeting precision to a Pearson correlation coefficient of 0.91, enabling a therapeutic-monitoring closed loop through long-term imaging. The MNBS PS designed by Xiong et al.[92] triggers ferroptosis by specifically targeting lipid droplets, with an enhanced type I ROS yield compared with conventional systems, unveiling a novel correlation between organelle localization and the regulation of cell death modalities. Feng et al.[93] have transcended the functional limitations of traditional single-targeting approaches with their OTBS-FR-ER self-assembling peptide. By targeting the ER and undergoing ordered nanofiber assembly, this peptide enhances ROS generation efficiency and triggers an ROS/ reactive nitrogen species (RNS) cascade reaction, leading to upregulated GRP78 expression and successfully activating robust type II immunogenic cell death (ICD). The THTTPy-PTSA probe, developed by Wang et al.[85] (Figure 3D), represents a more significant breakthrough. Initially designed by incorporating PTSA for ER targeting, this probe undergoes photo-oxidative dehydrogenation of its tetrahydropyridine group upon light irradiation, converting it into a pyridine group that subsequently functions as a mitochondrial-targeting moiety. This dynamic targeting mechanism enables the probe to migrate intelligently from the ER to mitochondria, thereby spatiotemporally amplifying oxidative stress and calcium signaling within both organelles. The resulting effects include elevated expression of ER stress markers (*p*-PERK/*p*-eIF2α), decreased mitochondrial membrane potential, and ultimately, activation of a robust immune response. Through modular design, these sophisticated single-targeting systems can function independently as therapeutic units or be flexibly assembled into multitargeting platforms, establishing an iterative cycle of "basic optimization → combinatorial innovation → re-optimization."

Currently, this field has forged a synergistic evolutionary trajectory for targeting strategies: single-targeting research serves as a cornerstone, providing molecular probes and mechanistic blueprints for multitarget synergism. Breakthroughs in dual-targeting approaches, in turn, inversely propel the intelligent and functional evolution of single-targeting systems. Furthermore, novel single-targeting technologies lay the groundwork for more intricate multitargeting designs. In the future, it is essential to transition from "empirical combinations" to "systematic regulation" by leveraging artificial intelligence (AI)-assisted optimization of targeting ligand combinations, dynamic dissection of interorganelle signaling crosstalk, and the development of carriers with enhanced metabolic stability. This transformative shift will usher tumor phototherapy into a new epoch of precision medicine[94].

3.2.2 Photoactive materials for tumor microenvironment modulation

The TME exhibits dynamic heterogeneity, resembling a complex pathological network. It is characterized by hypoxia, acidity, elevated interstitial fluid pressure, and immunosuppression, which collectively pose significant barriers to effective tumor therapy (Figure 4)[95,96]. The advent of photoactive materials is revolutionizing the paradigm of tumor treatment by converting the pathological characteristics of the TME, which once posed therapeutic resistance, into strategic points for precise intervention. This is achieved through intelligent molecular-level design and systematic dynamic regulation[97,98].

Within the hypoxic TME, the oxygen-dependent mechanism of traditional PDT faces fundamental challenges. However, innovative strategies involving nanomaterials have opened up bidirectional pathways to address these challenges. Zhang et al.[99] engineered TPASIC-PFH@PLGA NPs, which are loaded with liquid perfluorohexane (PFH). Upon exposure to NIR light, these NPs undergo a liquid-to-gas phase transition. This process not only releases stored oxygen to alleviate local hypoxia but also forms dense aggregates through nanostructural reorganization, significantly enhancing the ROS generation efficiency of the PS in its aggregated state. This "self-oxygenation-enhancement" dual-mode strategy transforms PDT's oxygen requirement from passive dependence to active supply (Figure 5A). For the deeply seated tumor regions experiencing extreme hypoxia, Zhou et al.[100] have advanced a novel strategy for targeting hypoxic tumor cores through their BT-LRC nanosystem. This system exploits an electron transfer cascade between the BODIPY-tetraphenylethylene (TPE) fluorophore and camptothecin, enabling direct production of type I ROS in HepG2 cells under severe hypoxia (Figure 5B). Concurrently, it releases DNA-damaging therapeutics, establishing an oxygen-independent "type I photodynamic-chemotherapy" synergistic network. This technological advancement from "oxygen supplementation" to "bypassing oxygen dependence" aligns closely at the molecular level with the NIR-BN nanosystem developed by Shi et al.[101] This material possesses an exceptionally small singlet–triplet energy gap (ΔE_{ST} = 0.09 eV) and a high molar extinction coefficient (3.3×10^4 M^{-1} cm^{-1}), ensuring efficient intersystem crossing (ISC). Its twisted molecular configuration induces multimodal structural relaxation upon photoexcitation, endowing the NIR-BN NPs with a photothermal conversion efficiency exceeding 50%. Crucially, intense intramolecular dihedral angle vibrations in the excited state enable the direct generation of highly toxic superoxide anion radicals ($\cdot O_2^-$) under 660 nm laser irradiation, thereby bypassing the dependence on molecular oxygen inherent in conventional PDT. This unique molecular mechanism provides an innovative paradigm for oxygen-independent synergistic PTT/PDT of deep-seated tumors. After nanomaterials surmount the hypoxia barrier within the TME, the acidic characteristics of the TME emerge as a new focal point for intervention. The pH of tumor tissues is typically lower than that of normal tissues (pH 6.5 to 7.0 versus 7.4), providing a rationale for the design of pH-responsive photoactive materials[102]. These materials often incorporate pH-sensitive chemical bonds or groups, including hydrazone bonds, imine bonds, and carboxylic acid groups. These components undergo cleavage or conformational changes in acidic environments, facilitating controlled drug release[103–105]. Dual-stimuli-responsive nanocarriers, which integrate pH-sensitive polymers with PSs, exhibit charge

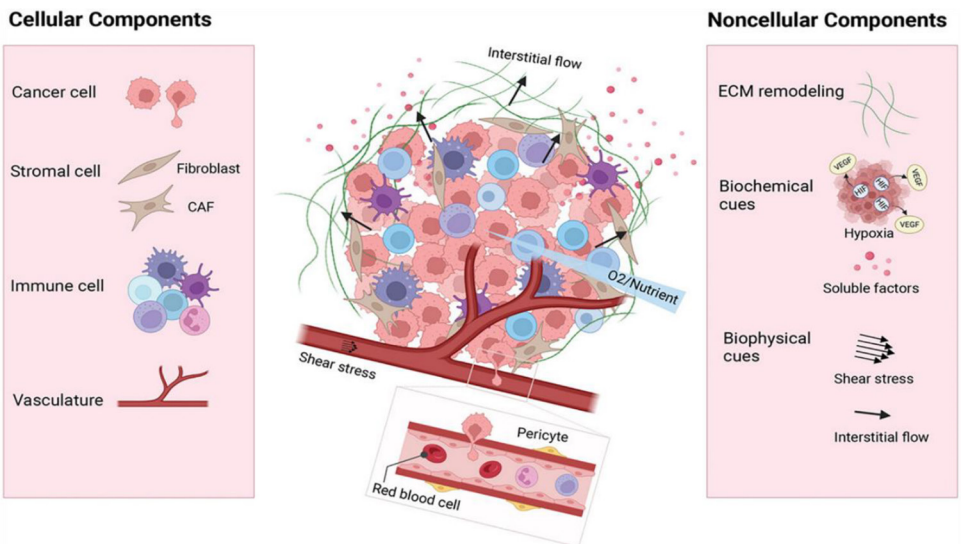

Figure 4. Schematic illustration of key components of the TME[95]. Copyright 2023, Wiley-VCH Verlag GmbH & Co. KGaA, Weinheim.

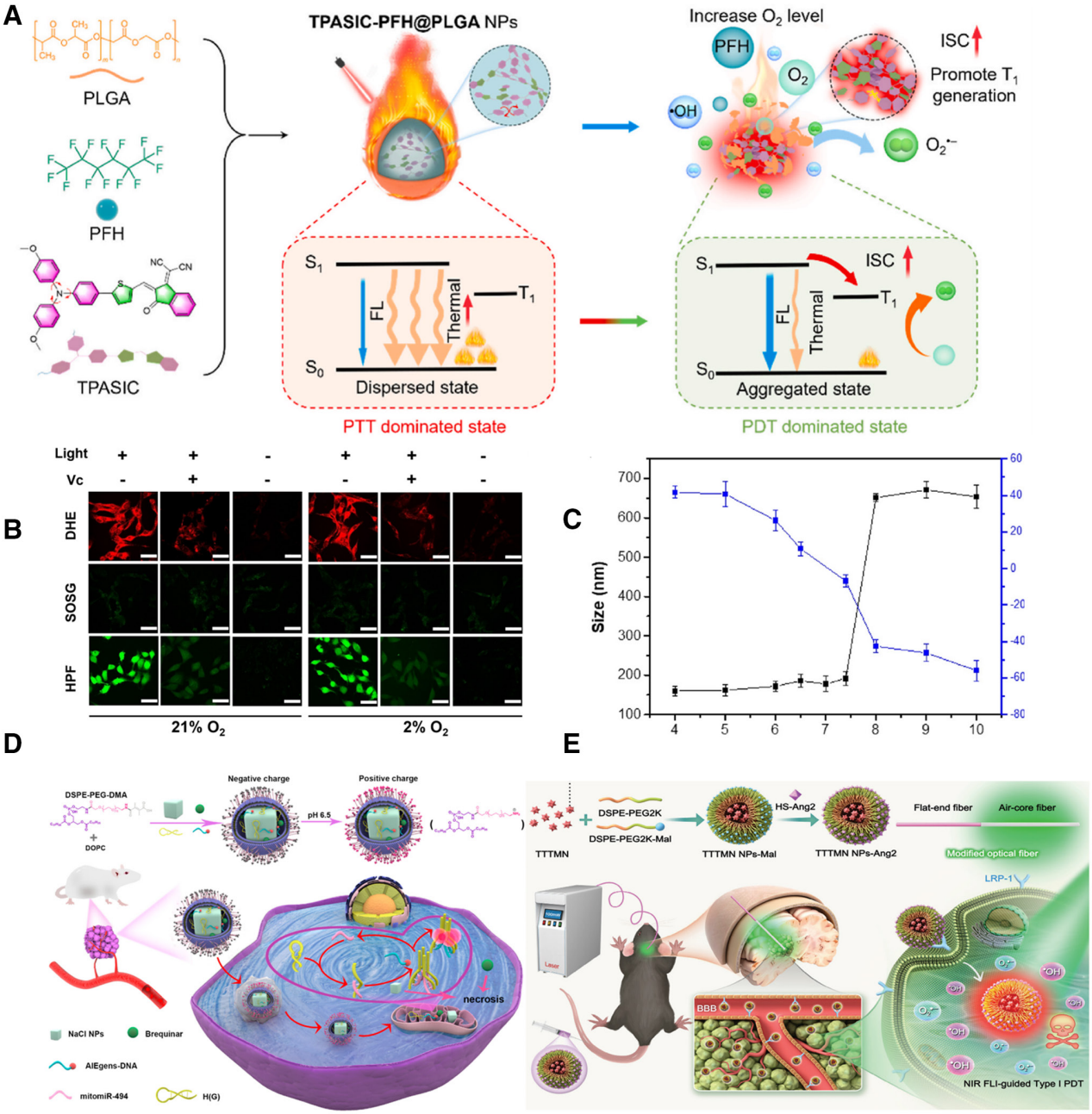

Figure 5. (A) Schematic illustration of the action mechanism of TPASIC-PFH@PLGA nanoparticles. Reproduced with permission from Ref[99]. Copyright 2025, Elsevier Ltd. (B) ROS detection in HepG2 cells under normoxic (21% O_2) and hypoxic (2% O_2) conditions, utilizing Dihydroethidium (DHE), Singlet Oxygen Sensor Green (SOSG), and Hydroxyphenyl Fluorescein (HPF) as fluorescence indicators for $\cdot O_2^-$, $^1O_2$, and ·OH, respectively. Scale bar: 50 μm[100]. Copyright 2024, Wiley-VCH Verlag GmbH & Co. KGaA, Weinheim. (C) pH-dependent variations in zeta potential and diameter of AIE-NPS[107]. Copyright 2020, Elsevier B.V. (D) Schematic Diagram of the Construction of NAB@DD-DC for mitomiR-494 Imaging and Ion-Interference Therapya[108]. Copyright 2024, American Chemical Society. (E) Synthesis and action mechanism diagram of TTTMN NPs-Ang2[109]. Copyright 2024, Wiley-VCH Verlag GmbH & Co. KGaA, Weinheim.

conversion under acidic or alkaline conditions through protonation and deprotonation mechanisms. These carriers also amplify the therapeutic efficacy of PTT or PDT upon light irradiation[106]. In the carrier-free HD-APNNA NPs with AIE characteristics designed by Cheng et al.[107], this concept is transformed into an intelligent responsive switch: protonation of carboxylic acid groups drives a reversal of surface charge from −5 to +10 mV (Figure 5C), accompanied by dynamic shrinkage of the NP size to 170 nm. This "acid-triggered dual response in morphology and function" not only enhances cellular membrane adsorption and tissue penetration but also achieves an ROS quantum yield of 56.7%, surpassing that of the clinical PS Ce6, while simultaneously avoiding the biological toxicity risks associated with exogenous carriers. This "acid-overcoming-acid" strategy is further expanded in a multidimensional manner in the NAB@DD-DC system developed by Du et al.[108] Here, pH-sensitive polymers hydrolyze in the acidic lysosomal environment, triggering charge reversal to facilitate lysosomal escape.

The released Na^+ disrupts mitochondrial membrane potential through osmotic pressure, concurrently activating mitochondrial-targeted imaging and pyrimidine metabolism blockade. This approach transforms the acidic microenvironment of the TME from a therapeutic obstacle into a spatiotemporal control node for precise delivery and synergistic therapy (Figure 5D).

The heightened interstitial fluid pressure and dense extracellular matrix (ECM) architecture within the TME have propelled innovative explorations in photoactive materials, employing physical–chemical synergistic strategies to breach barriers[110]. Using glioma as a representative model[111], the unique characteristics of its microenvironment further exacerbate therapeutic challenges: the blood–brain barrier (BBB) strictly impedes drug penetration[112,113], deep-seated infiltrative lesions are difficult to excite PSs due to tissue light attenuation[114], and hypoxic regions induced by rapid tumor proliferation directly attenuate the oxidative cytotoxic effects of conventional PDT[115]. To address this multidimensional barrier system, Xu et al.[109] and Zhang et al.[116] have proposed groundbreaking solutions. The former achieves reversible BBB opening and precise light-controlled therapy at a depth of 940 μm by combining focused ultrasound with a 2-photon-excitable NIR-II PS, enabling the simultaneous generation of both type I and type II ROS to cope with oxygen gradient heterogeneity. The latter designs an Angiopep-2 receptor-targeted type I PS and utilizes an air-core modified optical fiber to deliver laser light in situ to the tumor core, efficiently generating hydroxyl radicals (·OH) and superoxide anions ($\cdot O_2^-$) within a depth of 25 mm, thereby surmounting the limitations imposed by the hypoxic microenvironment (Figure 5E). The 2 strategies, centered on "physical modulation-deep energy delivery" and "biological navigation-in situ excitation," systematically dismantle the "barrier-hypoxia-light attenuation" dilemma in the glioma microenvironment, providing clinically translatable technical paradigms that combine precision and versatility. Within the technological pursuit of targeting the TME, photoactive materials are evolving from passive adaptation strategies to proactive architectural designs[117]. These advanced materials possess the capability to monitor multifaceted physiological variables, including hypoxia, acidity, and mechanical stress in real time, while concurrently converting pathological traits into therapeutic impetus through intricate molecular engineering. Specifically, phase-change substances restore oxygen homeostasis, protonation-responsive mechanisms bypass delivery impediments, electron transport systems override oxygen limitations, and mechanochemical interactions redefine immune dynamics[118–122]. Looking ahead, these dynamic regulatory systems may integrate optogenetic elements to achieve synergistic gene–microenvironment editing. Additionally, AI-driven closed-loop feedback mechanisms could optimize therapeutic parameters in real time. Furthermore, these systems might construct "energy hijacking" networks by exploiting tumor metabolic reprogramming. The evolution of nanomaterials from mere microenvironment decoders to proactive microenvironment architects signifies a transformative leap in tumor therapy, transcending conventional boundaries of localized cytotoxic effects and embarking on a novel epoch of systemic modulation. This paradigm shift not only necessitates a profound interdisciplinary dialogue between materials science and synthetic biology but also demands a precise reconstruction of the dynamic interplay within the TME using biomimetic models such as organoids and organ-on-a-chip platforms. Ultimately, this will facilitate the elevation of therapeutic strategies from molecular interventions to systemic remodeling, marking a significant advancement in cancer treatment.

3.2.3 Wavelength-tunable photoactive materials

In the field of precision tumor diagnosis and therapy, the evolution of photoactive materials is undergoing a paradigm shift from functional hybridization approaches to intelligent integration systems. The traditional "All-in-One" strategy, which combines diagnostic and therapeutic platforms (e.g., fluorescent dyes and PSs) through physical or chemical hybridization of multiple components, has facilitated multifunctional platform development. However, its clinical translation is severely impeded by challenges such as poor batch reproducibility, with a coefficient of variation frequently surpassing 15%, and unpredictable pharmacokinetics resulting from complex inter-component interactions[123–125]. This predicament has spurred the advancement of novel phototheranostic systems leveraging the AIE mechanism. The core of these systems lies in establishing a delicate balance between radiative and nonradiative decay pathways through intramolecular energy regulation, thereby integrating imaging and therapeutic functionalities within a single molecular species[126]. Compared with traditional materials, AIE materials not only streamline the preparation process by 3- to 5-fold but also exhibit well-defined structural characterization and optimized biocompatibility, demonstrating disruptive potential for clinical applications[127–129]. This innovative paradigm successfully overcomes the aggregation-caused quenching (ACQ) effect observed in traditional dyes. Leveraging the low tissue scattering, weak absorption, and high penetration depth characteristics of NIR light (700–1700 nm), AIE materials provide a technological foundation for the diagnosis and treatment of deep-seated tumors[130,131]. The technological evolution of NIR-I (700–900 nm) AIE probes follows a paradigm shift trajectory of "functional expansion—mechanistic innovation—technological leapfrogging," progressively advancing from foundational imaging to ultrahigh-resolution dynamic observation[132].

Early-stage breakthroughs targeted metabolic limitations of conventional probes. The DPPM-TPA NPs developed by Han et al.[133] employ a donor–acceptor–donor symmetric architecture (diphenylamino donor/DPPM core acceptor), achieving NIR absorption at 475 nm and emission at 585 nm. By leveraging 2-photon excitation technology, these NPs extended the in vivo tumor fluorescence tracking period to 9 days (Figure 6A), establishing a foundation for long-term imaging. Subsequent research prioritized theranostic integration, as exemplified by the TTCBTA NPs pioneered by Ma et al.[134]. These NPs are based on a donor–acceptor structural design (triphenylamine as the electron donor and benzothiazole as the electron acceptor), with molecules exhibiting highly twisted conformations. This spatial steric hindrance effectively suppresses π–π stacking interactions, reducing nonradiative decay pathways in aggregated states and thereby overcoming ACQ phenomena. Additionally, the strong intramolecular charge-transfer characteristics induce significant structural relaxation and solvent reorganization upon excitation, resulting in a substantial reduction in excited-state energy and a large Stokes shift of up to 230 nm. This significant spectral separation effectively reduces interference from fluorescence self-absorption and spontaneous fluorescence from biological tissues, enhancing signal penetration capability and facilitating high-contrast imaging of deep tissues. Concurrently, Yan et al.[135] designed a water-soluble AIE material, PEGTPA-NSD with enhanced biocompatibility, facilitating prompt signal accumulation in models of breast cancer bone metastasis. The structural features of PEGTPA-NSD indicated its potential for extended emission into the NIR-II region,

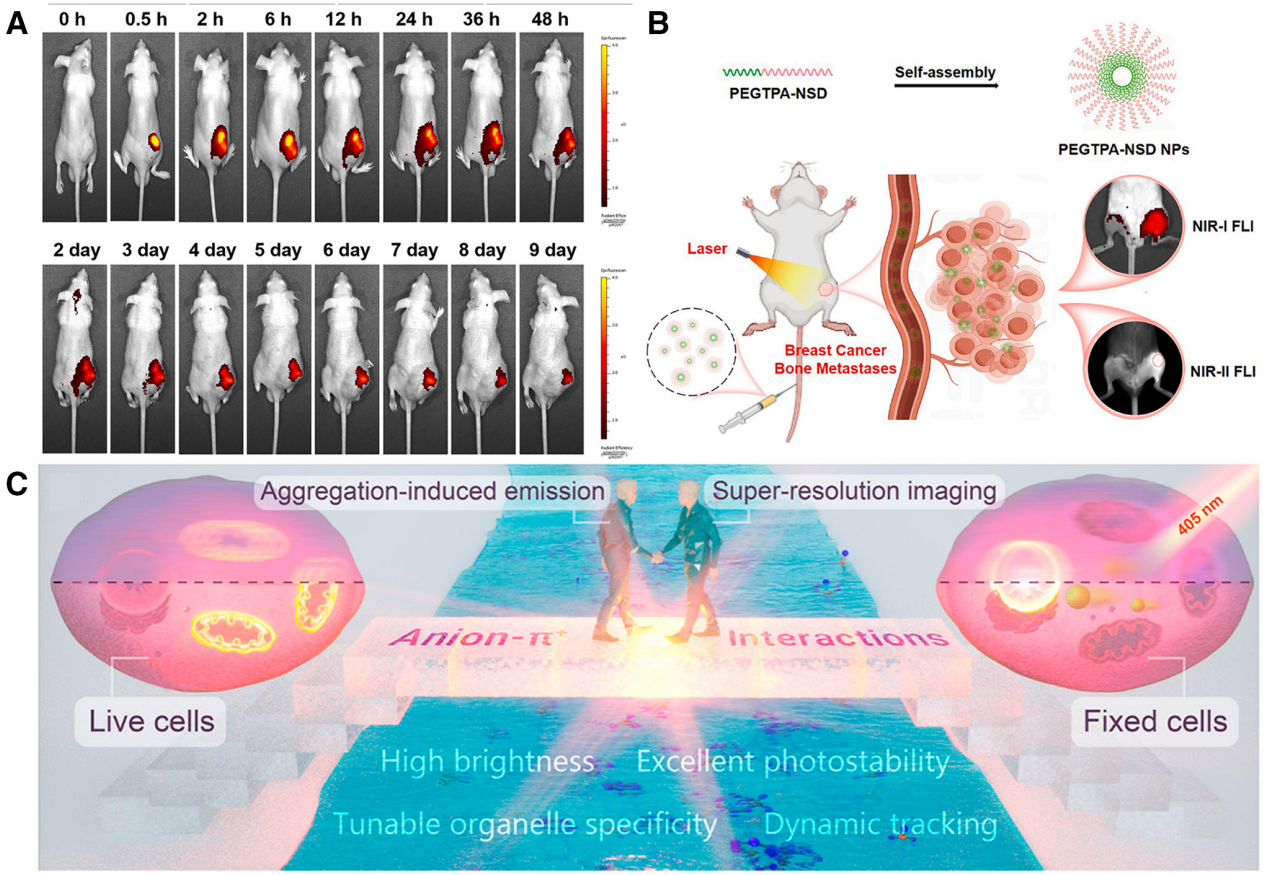

Figure 6. (A) In vivo fuorescent images of BALB/c nude mice (n = 3) intratumor injected with DPPM-TPA NPs[133]. Copyright 2024, Elsevier B.V. (B) Application of PEGTPA-NSD in tumor imaging[135]. Copyright 2025, Elsevier B.V. (C) Chemical structures and optical performance of these developed AIEgens. Schematic illustration of DTPAP-P fort unable organelle-specific imaging and dynamic tracking in ultrahigh resolution[137]. Copyright 2022, American Chemical Society.

motivating preliminary investigations into NIR-II imaging applications (Figure 6B). Building on functional integration, Barman et al.[136] advanced a luminescent mechanism innovation by integrating AIE characteristics with thermally activated delayed fluorescence, engineering BTMCz NPs. These NPs significantly improved PS imaging contrast and therapeutic efficacy at the photophysical level, offering theoretical support for super-resolution advancements. Ultimately, Xu et al.[137] successfully enhanced the solid-state photoluminescence quantum yield of their cationic AIEgen, DTPAP-P, to 35.04% by implementing a dual-pathway strategy that suppresses molecular motion. The 700 nm emission peak, combined with stimulated emission depletion nanoscopy, enhanced mitochondrial imaging resolution from 1028 to 165 nm. It also introduced a light-controllable targeting switch mechanism, enabling dynamic tracking of mitochondrial fission–fusion in live cells at 165 nm resolution and nucleolar migration for super-resolution imaging in fixed cells at 184 nm (Figure 6C). This advancement addresses clinical needs for "prolonged visualization and precise intervention" while revealing, through spatiotemporally controlled nanoscale observation, molecular-scale interactions between mitochondria and nuclei for the first time. Consequently, this represents a transformative shift of AIE probes from theranostic tools to decoders of organelle interactions. However, NIR-I imaging is limited by inadequate tissue penetration depth (<3 mm) and significant signal attenuation (>50%) in deep tumors. Furthermore, challenges such as photobleaching and background noise interference hinder the accurate detection of small lesions (<2 mm)[138]. Consequently, research has increasingly focused on the second NIR-II (1000–1700 nm), which offers superior penetration capabilities. The photon scattering coefficient in the NIR-II region is reduced by 2 to 3 orders of magnitude compared with NIR-I, enabling penetration depths exceeding 5 mm. Additionally, autofluorescence from biological tissues is significantly diminished in this range, substantially improving the signal-to-background ratio (SBR) in imaging[139].

In recent years, multimodal theranostic systems based on NIR-II AIE materials have achieved significant advancements due to breakthroughs in molecular engineering. Research now focuses on the precise modulation of emission wavelengths and the synergistic enhancement of diagnostic and therapeutic functionalities[140,141]. From the perspective of the technological evolution trajectory, where emission wavelengths progressively shift from shorter to longer regions, various research teams have advanced through innovative molecular design strategies, systematically overcoming bottlenecks in deep-tissue imaging and synergistic therapy. A landmark achievement in the short-wavelength NIR-II region (900–950 nm) was reported by Jin et al.[142], who developed SFX-IC NPs. They employed a spirocyclic functionalization strategy to develop organic PSs with an emission peak precisely positioned at 935 nm when excited by an 808 nm laser. These PSs exhibited a fluorescence brightness 1.74-fold higher than that of the commercially available ICG. This molecular engineering not only achieved fluorescence

imaging with a high SBR of >4.2, significantly enhancing imaging clarity and accuracy, but also integrated multimodal imaging capabilities, including PAI and PTI, enabling multidimensional and complementary biomedical monitoring. Moreover, the rigid spirocyclic structure effectively suppressed nonradiative transitions, providing a new paradigm for the precise localization of deep-seated tumors (e.g., subcutaneous lesions at 7 mm). This achievement laid an important foundation for the subsequent development of longer-wavelength probes. Next, Zheng et al.[143] successfully extended the emission wavelength to 950 nm through a synergistic approach in receptor engineering and sulfur atom embedding technology. The designed 4TPQ NPs demonstrated excellent fluorescence properties while strategically leveraging the heavy-atom effect of sulfur atoms and the charge-transfer characteristics of the receptor units. These design elements enhanced ROS generation efficiency and achieved a photothermal conversion efficiency of 32.5%. This dual-functionalized "imaging-therapy" design exhibited unique advantages in a mouse model of breast cancer bone metastasis. NIR-II fluorescence guidance accurately localized micrometastases, while the synergistic photothermal and PDT reduced tumor volume, forming a complete technological chain from molecular design to clinical translation. Along the technological route of wavelength extension, Zhang et al.[144] further pushed the emission wavelength to 992 nm through an intramolecular motion regulation strategy, constructing the breakthrough TSSI NP system. This material exhibits multiple advantages in the far-end NIR-II region (>950 nm): first, its NIR-II fluorescence imaging SBR is enhanced, enabling the detection of minute tumors (<2 mm) that are difficult to identify with traditional methods; second, the material's unique dual-channel energy conversion mechanism allows for high-resolution imaging of tumor microvascular networks through PAI and synergistic tumor-killing effects through PTT and PDT under NIR excitation. Notably, the PTI functional module enables real-time monitoring of the temperature field distribution in the treatment area, providing a dynamic feedback mechanism for precise control of photothermal conversion efficiency (Figure 7A). In the 4T1 breast cancer model, this multimodal synergistic mechanism achieved a dynamic closed loop for real-time monitoring of therapeutic responses and efficacy evaluation, marking a new stage in the advancement of "theranostic integration" technology. These 3 typical cases present a clear evolutionary logic: from the short-wavelength high-brightness imaging of SFX-IC to the treatment-enhancing mid-wavelength 4TPQ, and then to the long-wavelength multimodal fusion of TSSI. The researchers have systematically addressed the challenges of balancing tissue penetration depth, therapeutic efficiency, and imaging accuracy through iterative innovations in molecular engineering. This design philosophy of wavelength-function synergistic optimization provides a crucial paradigmatic reference for the future development of intelligent theranostic platforms.

Building on the aforementioned research, You et al.[145] developed the 4TT-PBPT AIEgen utilizing N-heterocyclic fused-ring design, pushing the emission wavelength to 1026 nm. This material not only enables millimeter-level localization of in situ bladder tumors through trimodal imaging (NIR-II FLI/PAI/PTI) but also achieves a photothermal conversion efficiency of 73.8% at 100 μM, approaching the theoretical limit of gold NPs. Combined with the ROS-mediated apoptosis mechanism, it attains a tumor ablation rate exceeding 95% (Figure 7B, C). This innovation in the fused-ring system significantly enhances material stability and functional density, opening up new avenues for the design of ultralong-wavelength probes. As the emission wavelength extends further into longer spectral regions, the BETT-2 AIE molecule developed by Song et al.[146] exhibits an emission peak at 1240 nm. This material efficiently generates superoxide radicals (O_2^-) through the type I photodynamic pathway, while simultaneously achieving a photothermal efficiency of 56.6%. Its multimodal imaging system enables dynamic analysis of TME heterogeneity, providing novel insights for addressing the challenges of energy delivery to deep-seated tumors. More cutting-edge is the "inside-out" phototherapy strategy proposed by Zhang et al.[147], which integrates NIR-II AIEgens with modified optical fibers (Figure 7D). By introducing heavy atoms and strong donor–acceptor interactions and highly twisted conformations, the molecule exhibits NIR-II fluorescence emission (1092 nm), efficient photothermal conversion (η = 58.9%), and photodynamic effects, and photodynamic effects primarily generating hydroxyl and superoxide radicals under 808 nm excitation. NPs surface-modified with the iRGD peptide (NPs-iRGD) are capable of targeted enrichment at tumor sites, and modified optical fibers, comprising a fused flat-end fiber and an air-core fiber, are utilized to deliver light energy to deep tissues. Furthermore, this strategy maintains efficient photothermal/photodynamic effects in skin barrier simulation experiments, demonstrating its potential for clinical translation.

In recent years, photoactive materials excited in the second NIR-II have revolutionized tumor vascular imaging technology, leveraging their exceptional deep-tissue penetration and precise optical tomography capabilities. Through synergistic innovations in molecular engineering and nonlinear optics, researchers have constructed multimodal imaging probe systems, achieving stepwise breakthroughs in imaging depth, spatiotemporal resolution, and functional visualization. The pioneering work in this field was conducted by Li et al.[148], who developed the NIR-II AIE luminogenic DCTBT. By precisely tuning the electron-donor structure, this probe achieved unprecedented brain imaging depths of 2180 μm (with skull removed) and 1135 μm (intact skull) under 1700 nm 2-photon excitation. Boasting a large 2-photon action cross-section of 1.2 GM and retaining 90% of fluorescence, it not only sets new records for penetration depth among organic probes but also facilitates the effective monitoring of cerebrovascular hemodynamics at a depth of 714 μm, laying a technological foundation for studying deep-seated tumor vasculature (Figure 8A). This breakthrough has spurred interdisciplinary investigations into multidimensional imaging, notably culminating in the seminal work of Gong et al.[149], who achieved a pivotal advancement in 3-dimensional (3D) quantitative analysis. They developed HA@TANP NPs, leveraging synergistic temperature-controlled polymerization and optical clearing techniques to facilitate 3D panoramic reconstruction of the vascular network in metastatic lung cancer models. Achieving a spatial resolution surpassing the 5 μm limit, this system allows precise quantification of dynamic changes in vascular diameter (4–55 μm), length (25–75 μm), and morphological straightness (0.899–0.914). This advancement has propelled the study of tumor vascular heterogeneity from 2D observational paradigms into a new era of 3D quantitative analysis.

With the advancement of 2PF techniques, 3PMhas emerged as a transformative tool. It capitalizes on the enhanced deep-tissue penetration capabilities of the NIR-III excitation window, effectively addressing the depth limitations inherent in 2PF for in vivo brain imaging. Early research efforts have centered on the development of noninvasive probes. For example, Qin et al.[151] designed the AIE molecule—BTF, devoid of a traditional

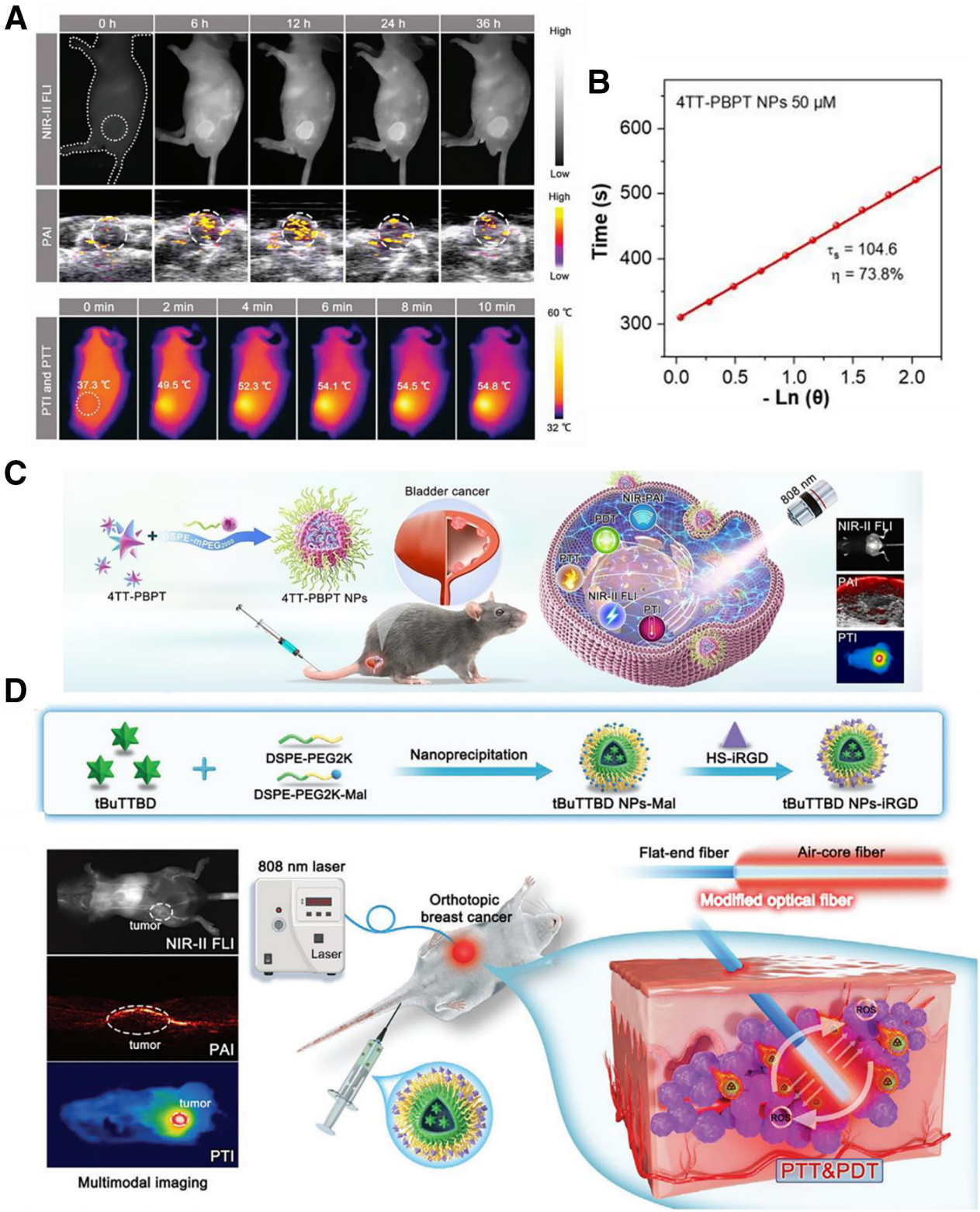

Figure 7. (A) In vivo multimodal imaging-guided synergistic therapeutic efficacy of TSSI NPs on 4T1 tumor-bearing BALB/c nude mice via systemic administration[144]. Copyright 2020, Wiley-VCH Verlag GmbH & Co. KGaA, Weinheim. (B) Calculation results of the photothermal conversion efficiency of 4TT-PBPT NPs[145]. Copyright 2024, Wiley-VCH Verlag GmbH & Co. KGaA, Weinheim. (C) The preparation process 4TT-PBPT NPs and applications in multimodal imaging-guided orthotopic bladder cancer phototherapy[145]. Copyright 2024, Wiley-VCH Verlag GmbH & Co. KGaA, Weinheim. (D) Synthesis of tBuTTBD NPs-iRGD and interstitial light beam-mediated phototherapy guided by trimodal imaging[147]. Copyright 2024, Wiley-VCH Verlag GmbH & Co. KGaA, Weinheim.

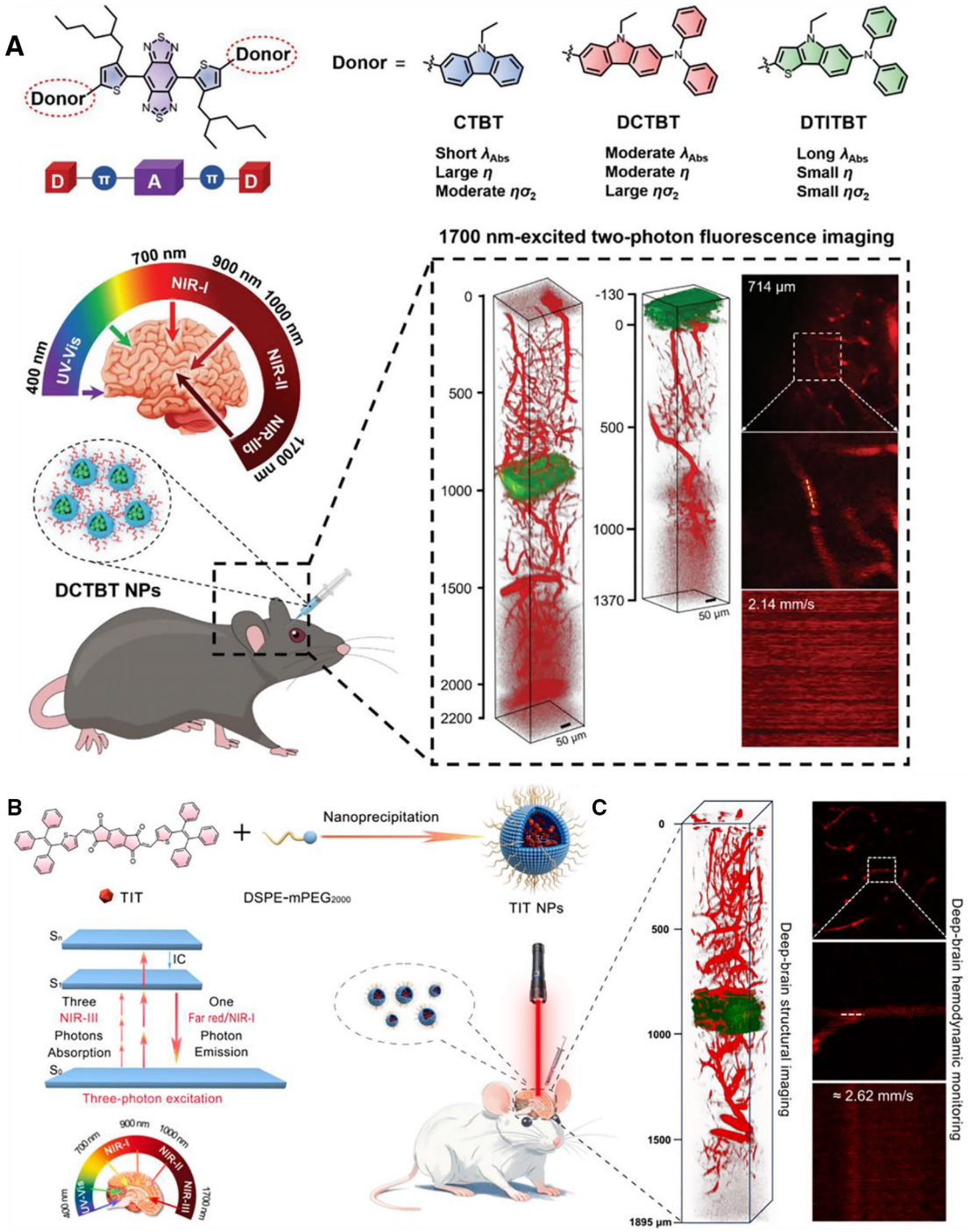

Figure 8. (A) Schematic illustration of electron donor engineering for fluorophores, and applications in deep brain structural and hemodynamic 2PFimaging excited at the 1700 nm window[148]. Copyright 2023, Wiley-VCH Verlag GmbH & Co. KGaA, Weinheim. (B) Preparation of TIT NPs and schematic illustration of the application of TIT-NPs in 3PM imaging of deep cerebral vessels in mice after craniotomy. (C) and hemodynamic monitoring with 1665 nm wavelength excitation (right)[150]. Copyright 2024, Elsevier B.V.

TPE backbone, which exhibits a large 3-photon absorption cross-section of 2.56×10^{-79} cm^6 s^2 under 1550 nm excitation. High-quantum-yield (36.1%) probes were prepared using a nanoprecipitation method. This groundbreaking work enabled 3D imaging of the cerebrovascular network beneath intact skulls (penetration depth: 900 μm), facilitating the first noninvasive monitoring of cerebral thrombosis formation and providing an in situ observational tool for cerebrovascular pathology research. Advancements in molecular engineering have propelled the performance limits of 3-photon fluorescence probes to new heights. Yang et al.[150] optimized an AIEgen—TIT, featuring a symmetric donor–acceptor–donor configuration that precisely couples planar electron acceptors with twisted donor units. Under 1665 nm excitation, TIT achieves a 3-photon action cross-section ($\eta\sigma_3$) of 603×10^{-84} cm^6 s^2 photon^{-2}. In cranial window models, the probe achieves an imaging depth of 1895

μm and enables dynamic tracking of hemodynamics at depths up to 1200 μm (Figure 8B, C). Compared with the earlier BTF system, TIT enhances NIR-III excitation efficiency by an order of magnitude through a delicate balance of π-conjugation extension and molecular motion suppression, marking a paradigm shift from "structural observation" to "functional analysis" in deep-brain imaging.

The evolution from depth breakthroughs in 2-photon microscopy to multidimensional analysis enabled by 3-photon microscopy represents a significant technological trajectory, characterized by the deep integration of NIR materials and nonlinear optics. Current research not only uncovers in situ characteristics of aberrant vascular branching and leakage within TMEs through advanced optical tomography capabilities but also paves the way for theranostic integration via modular probe design. By integrating targeting recognition and therapeutic functional units, these intelligent nanoprobes hold promise for realizing closed-loop diagnostics and therapeutics—spanning from vascular anomaly detection to precision drug delivery. This development propels the field of precision oncology into a new era of molecular dynamics manipulation, heralding transformative possibilities for personalized cancer treatment.

3.2.4 Photoactive materials for combined immunotherapy strategies

Immunotherapy constitutes a revolutionary approach in oncology, achieving antitumor effects by activating the body's immune system[152]. Among these approaches, immune checkpoint blockade therapy stands out for its mechanism of interrupting immunosuppressive pathways such as PD-1/PD-L1. This approach markedly augments the antitumor activity of T cells and has demonstrated remarkable efficacy in treating malignancies like melanoma and non–small cell lung cancer[153–155]. However, the systemic administration of traditional monoclonal antibodies frequently triggers immune-related adverse reactions and struggles to overcome the immunosuppressive characteristics of the TME. This has prompted researchers to explore more targeted and synergistic combination therapy strategies[156–158]. Phototherapy-induced ICD offers a novel approach to circumvent these limitations[159]. By triggering the release of danger signals such as calreticulin (CRT), high mobility group box 1 protein (HMGB1), and ATP from tumor cells through PDT or PTT, DCs can be activated and antigen presentation enhanced, thereby strengthening systemic antitumor immune responses[160–163].

The technological evolution of photoimmunotherapy has unfolded through a series of progressive breakthroughs, structured across 4 interconnected dimensions: local ablation, systemic activation, precise modulation, and multimodal synergy. During the initial mechanistic investigation, Liu et al.[164] developed the BSA/TPA-Erdn nanosystem, capitalizing on their distinctive photophysical characteristics. They validated the release of danger signals such as CRT and HMGB1 mediated by ROS via utilizing the NSG mouse models. This confirms the primary immune activation effects of PDT-induced DC maturation and T-cell infiltration (Figure 9A). This study established the molecular design foundations of photoimmunotherapy. However, constrained by its unimodal therapeutic mechanism, the induced ICD effect had not yet breached the physical barriers of the TME. The TPETTBI molecule proposed by Yang et al.[165] marked a pivotal technological breakthrough. Through molecular engineering, they integrated mitochondrial-targeting modules with AIE-active groups, precisely localizing therapeutic targets to cellular energy hubs. This design achieved spatiotemporal synergy between efficient ROS generation (PDT) and NIR photothermal conversion (PTT). Experimental data demonstrated that this dual-strike strategy, targeting the mitochondrial microenvironment, amplified ICD effects 3.2-fold and successfully activated $CD8^+$ memory T-cell subsets, achieving a 67% inhibition rate for distant metastases in bilateral tumor-bearing models (Figure 9B–D). This multimodal synergistic mechanism addressed the issue of limited tissue penetration inherent in conventional phototherapies. Nonetheless, the study simultaneously revealed the limitations of ICD induction alone; although it effectively provokes immediate immune reactions, it struggles to reverse deep-seated immunosuppressive microenvironments characterized by tumor-associated macrophage polarization and regulatory T-cell infiltration.

Sun et al.[166] have pioneeringly integrated phototherapy with an artificial antigen-presenting system, propelling therapeutic strategies to actively stimulate immune responses. The developed saDC@Fs-NPs constructs super artificial DCs utilizing genetically engineered tumor cell membranes. These NPs not only induce ICD through PDT to release tumor antigens but also directly activate T cells via surface-expressed pMHC-I/CD86 molecules. Furthermore, they synergize with an anti-LAG3 antibody to alleviate immune checkpoint inhibition (Figure 10A). In the 4T1 breast cancer model, this design achieved a 3-fold increase in $CD8^+$ T-cell infiltration and activated the abscopal effect, indicating a transition from simple immune priming by phototherapy to active immune regulation. Subsequently, Zhang et al.[167] developed TPE-Ni/OPYO NPs, innovatively combining PTT with chemoimmunotherapy. This system precisely releases chemotherapeutic drugs through a 940 nm laser-triggered phase transition at 64 °C, employing the ICD effect induced by PTT to promote DC maturation to 89.9%. It achieves spatiotemporal synergy between physical ablation and chemoimmunotherapy, enhancing the abscopal tumor inhibition rate to 68% (Figure 10B).

Advancements in genetic engineering technologies have propelled the field of photoimmunotherapy, enabling a transformative progression from targeted delivery to multidimensional immune programming. Cui et al.[168] employed metabolic glycoengineering to genetically modify tumor cells, facilitating the overexpression of azide groups on their surface. Based on this study, they developed NP-DBD NPs carrying dibenzocyclooctyne (DBCO) ligands, achieving tumor-specific targeting through bioorthogonal click chemistry. Surface ligands optimized by clustered regularly interspaced short palindromic repeats (CRISPR) screening further elevated the NP enrichment rate in pancreatic cancer to 82%. Upon activation by an 808 nm laser, these NPs synchronously generate ROS with a quantum yield of 0.89 and induce double-strand breaks in both mitochondrial and nuclear DNA through the AIE effect. This innovation activates the cGAS-STING pathway, increasing the secretion of type I interferons compared with traditional PSs and laying the foundation for precise coupling between phototherapy and innate immunity (Figure 10C). Building on this, Cao et al.[169] employed lentivirus-mediated genetic recombination technology to transform DCs into bioreactors that continuously secrete DEV-AIE biomimetic exosomes carrying CRISPR interference elements targeting the *SOX2* gene. These exosomes, genetically engineered to display CD80/CD86-PD-L1 fusion proteins on their surface, can directly activate T-cell receptors. Concurrently, the internally loaded AIE PS specifically accumulates in the tumor stem cell microenvironment, reducing the proportion of

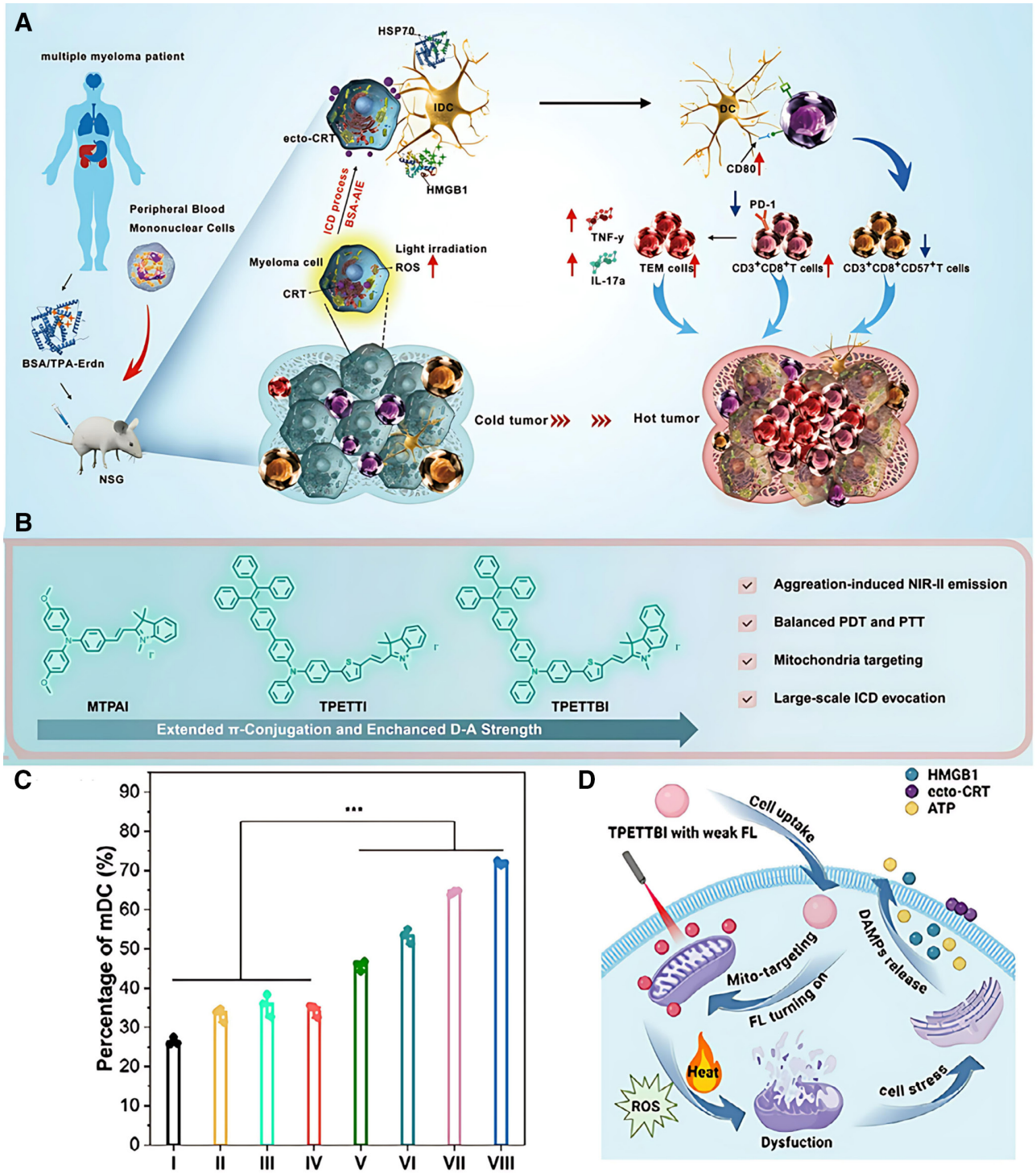

Figure 9. (A) Schematic illustration of BSA/TPA-Erdn-mediated ICD immunotherapy for multiple myeloma treatment[164]. Copyright 2022, Wiley-VCH Verlag GmbH & Co. KGaA, Weinheim. (B) Flow cytometry analysis of mature dendritic cells (CD80+CD86+, gated on CD11c+ cells). (C) Molecular Design Strategy for TPETTBI. (D) Schematic mechanism of TPETTBI-triggered immunogenic cell death (ICD) induction. Data are presented as mean ± standard deviation (n = 3). *** denotes $p < 0.001$[165]. Copyright 2025, Wiley-VCH Verlag GmbH & Co. KGaA, Weinheim.

CD44+/CD24+ cancer stem cells through photodynamic effects and achieving spatiotemporal synchronization between innate immune signaling and artificial phototherapy regulation (Figure 10D). Furthermore, Sun et al.[170] integrated multiple genetic editing strategies to develop the SEx@Fc-NPs engineered vesicle system. This system blocks the CD24 immune checkpoint using Siglec-10 nanobodies delivered by AAV vectors and continuously activates the gp96 molecule using CRISPRa technology to enhance antigen presentation efficiency. Combined with the PDT-induced conversion of M2 macrophages to the M1

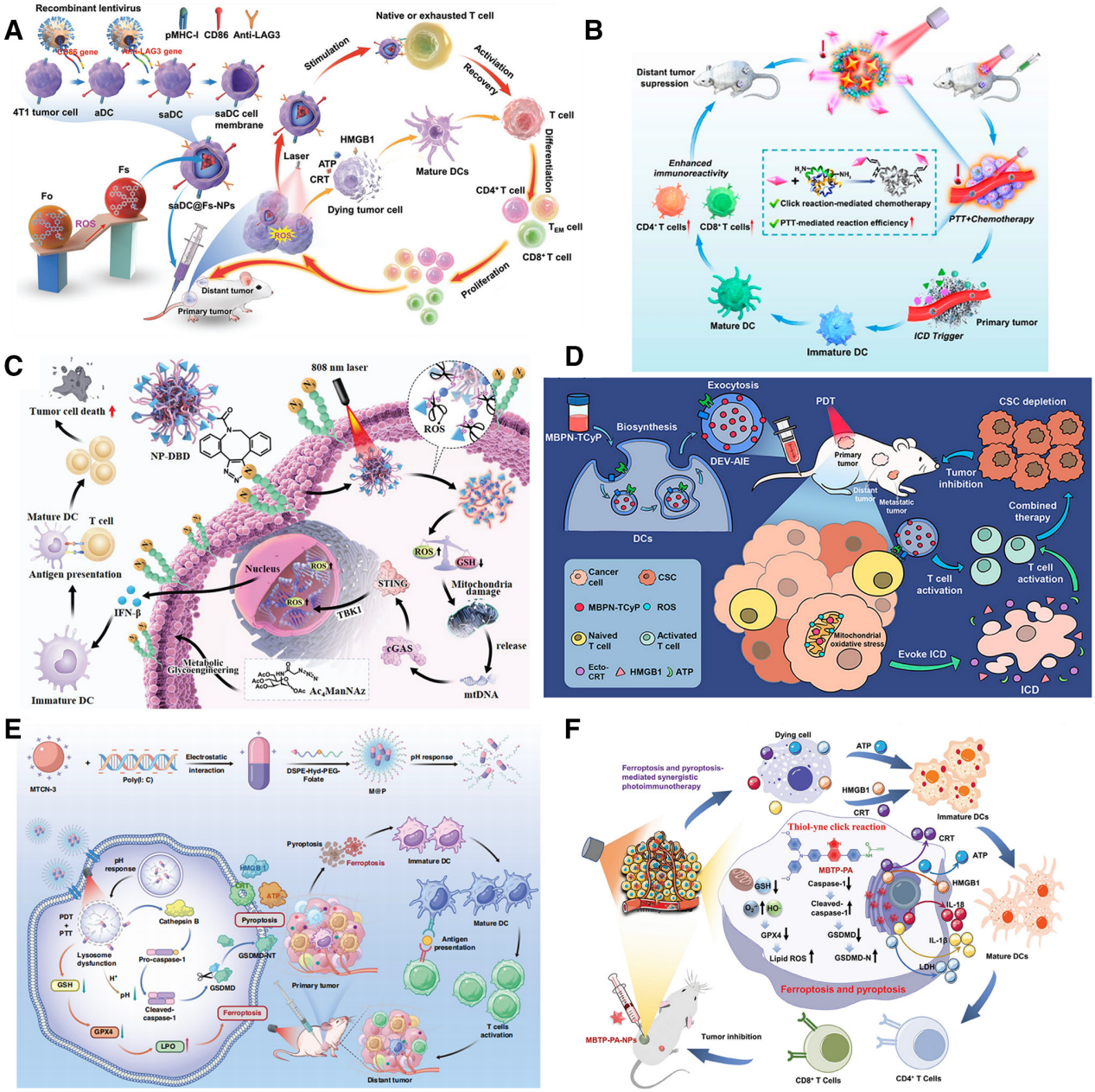

Figure 10. (A) saDC@Fs-NPs presented tumor antigens and reversed immunosuppression for PDT-enriched immunotherapy[166]. Copyright 2022, Wiley-VCH Verlag GmbH & Co. KGaA, Weinheim. (B) PE-Ni/OPYO NPs for synergistic cancer therapy by photothermal ablation and ICD of tumor cells[167]. Copyright 2023, American Chemical Society. (C) NP-DBD anchored into the membranes of cells pretreated with Ac4ManNAz via bioorthogonal copper-free click reaction to enhance the PDT/PTT/NIR-II FLI effect and activate the cGAS-STING pathway, leading to DC maturation and powerful antitumor immune responses[168]. Copyright 2023, Wiley-VCH Verlag GmbH & Co. KGaA, Weinheim. (D) Scheme of the biosynthetic DEV-AIE-NPs for synergistic photodynamic immunotherapy[169]. Copyright 2022, American Chemical Society. (E) Illustration of multifunctional nanoplatforms M@P inducing cancer cell pyroptosis and ferroptosis for cancer photoimmunotherapy[171]. Copyright 2025, Springer Nature. (F) Schematic illustrations of ferroptosis- and pyroptosis-mediated immunotherapy facilitated by the click reaction therapy and PDT[173]. Copyright 2025, Wiley-VCH Verlag GmbH & Co. KGaA, Weinheim.

phenotype, this system employs a 3D synergistic mechanism of immune remodeling-antigen release-checkpoint blockade. In a melanoma model, it maintained the proportion of central memory T cells above 35% for 42 days, establishing long-lasting cross-tumor immunologic memory with a single treatment. These 3 studies, through layered advancements in genetic editing technologies—ranging from targeted activation and cellular factory modification to the construction of systemic immune networks—collectively propel photoimmunotherapy into a new era of programmable, multitarget regulation. Recent research is accelerating the development of multimodal intelligent platforms, particularly in the field of photoimmunotherapy. Diverse research groups are contributing to this progress by exploring innovative approaches from multiple angles. For example, Wang et al.[171]. developed a M@P nanoplatform with pH-responsive lysosome-targeting characteristics, which was mainly formed through the self-assembly of an AIE PS (MTCN-3) and an immune adjuvant-Poly (I:C) M@P disrupts lysosomal function by

Table 1

Summary of selected molecules.

Molecular name	Molecular structure	Subcellular targeting	ROS type	References
TCF-Mem	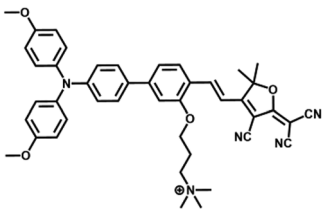	Cell membrane	I	[82]
DPITQ	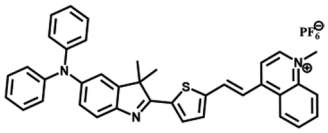	Cell membranes and mitochondria	I and II	[83]
BTZPP	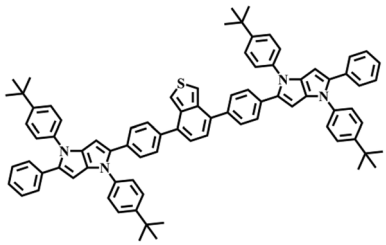	Lysosome	II	[91]
MNBS	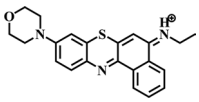	Lipid droplet	I	[92]
THTTPy-PTSA	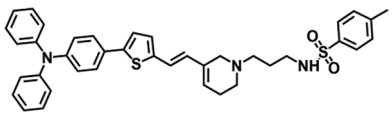	Endoplasmic reticulum and mitochondria	I	[85]

Molecular name	Molecular structure	Targeting the tumor microenvironment	ROS type	References
TPASIC	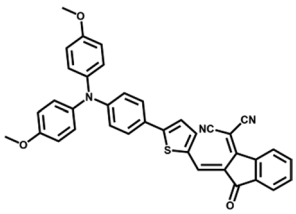	Hypoxic	I	[99]
NIR-BN	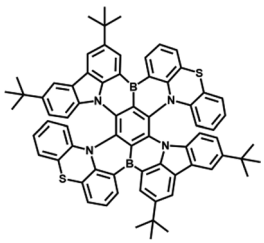	Hypoxic	I	[101]
HD-APNNA	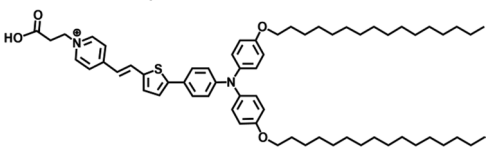	pH response	II	[107]

(Continued)

Table1

(Continued)

Molecular name	Molecular structure	$\lambda_{ex}/\lambda_{em}$ (nm)	ROS type	References
DPPM-TPA	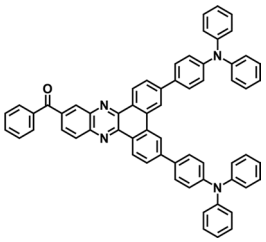	475/610	/	[133]
TTCBTA	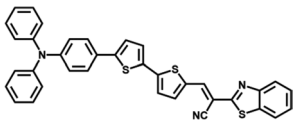	505/710	II	[134]
PEGTPA-NSD	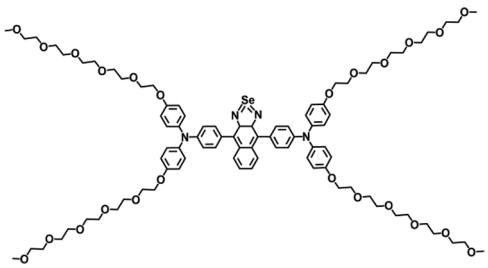	590/833	/	[135]
SFX-IC	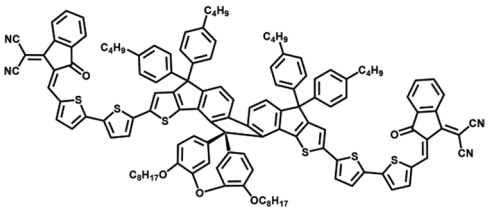	647/935	I and II	[142]
4TPQ	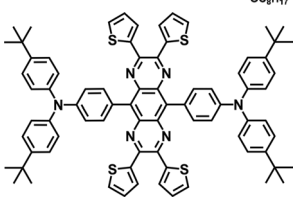	615/950	I	[143]
4TT-PBPT	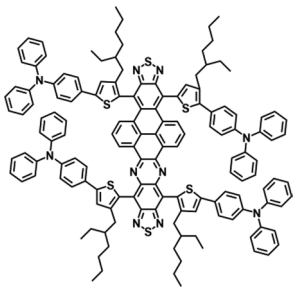	700/1026	/	[145]
BETT-2	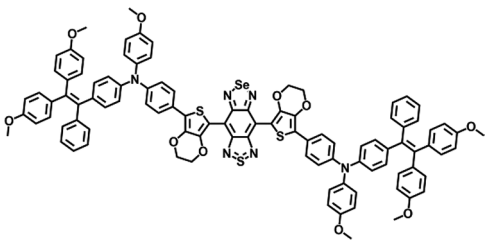	915/1024	I	[146]
tBuTTBD	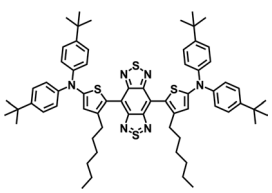	812/1088	I	[147]

"/" represents the type of uncertain reactive oxygen species.

generating ROS and local hyperthermia (56.6 °C) under 520 nm laser irradiation. Synchronously, it can induce pyroptosis [via the caspase-1/Gasdermin D (GSDMD) pathway] and ferroptosis (through GSH depletion and lipid peroxidation). This process releases DAMPs, including CRT and HMGB1, which activate DCs. By integrating lysosomal targeting, dual modes of cell death induction, and immune adjuvant synergy, this study overcomes the limitations of traditional phototherapy's single mechanism and marks a transition of photoimmunotherapy toward systematic regulation (Figure 10E). Following this research strategy, Li et al.[172] developed a CMNPs/PD-1 system, which attained novel breakthroughs in molecular modification and targeting mechanisms. This system innovatively integrates genetically engineered PD-1-modified cancer cell membrane vesicles (PD-1/CMNVs) with AOTTIT, a multimodal phototheranostic molecule with high absorption in the NIR-II window. The AOTTIT molecule, through an expansion of its π-conjugated architecture and strategic alkyl chain modifications, achieves a triad of functionalities: NIR-II fluorescence imaging with an emission maximum at 903 nm, a photothermal conversion efficiency of 64.74%, and type I PDT primarily mediated by hydroxyl radicals. PD-1/CMNVs significantly enhance tumor accumulation through dual mechanisms of homologous targeting and active PD-1/PD-L1 blockade. Building upon the explorations of the preceding teams, Wang et al.[173] make progress in therapeutic modal integration and immune memory induction. They developed an NIR-II responsive intelligent nanoplatform—MBTP-PA-NPs, which targets and depletes intracellular GSH via thiol-yne covalent reactions, thereby alleviating tumor hypoxia. This multifunctional platform combines type I PDT, PTT, and chemodynamic therapy. It activates the caspase-1/GSDMD-N pathway to induce pyroptosis and depletes GPX4 to trigger ferroptosis, enhancing the release of HMGB1 and ATP through dual cell death mechanisms (Figure 10F). These studies sequentially target critical mechanisms: enhancing immune activation via lysosomal targeting, amplifying immune responses through PD-1 blockade, and sustaining therapeutic effects via metabolic modulation. Collectively, they establish a comprehensive technological framework that spans lesion ablation, immune activation, and immune remodeling, advancing photoimmunotherapy into a new era of multimodal synergy and spatiotemporally precise regulation.

The technological progression in immunotherapy unfolds through 4 distinct stages: initial elucidation of the fundamental mechanisms underlying ICD, subsequent creation of artificial antigen-presenting systems, then advancement to genetically engineered biomimetic carriers, and ultimately culminating in the assembly of multimodal intelligent platforms[174,175]. Successive stages have surmounted the limitations of prior approaches, retaining phototherapy's fundamental benefits while advancing therapeutic scope through innovative delivery mechanisms and refined immune modulation. This evolution has culminated in a novel oncological treatment paradigm, harmoniously integrating spatiotemporal precision with systemic therapeutic synergy.

4. Conclusion and perspective

Recent advancements in AIEgens have significantly propelled their application in tumor diagnosis and therapy, capitalizing on distinctive photophysical characteristics. By meticulous molecular engineering, these materials circumvent the ACQ limitation encountered by conventional fluorophores at elevated concentrations. Furthermore, they facilitate a synergistic combination of multimodal imaging and phototherapeutic capabilities, providing a novel paradigm for precise tumor diagnosis and treatment. This review systematically elaborates on the innovative design strategies of photoactive materials based on AIE characteristics. Multidimensional synergistic designs are highlighted, including precise subcellular organelle targeting (e.g., mitochondria/lysosome-specific probes), dynamic responses to the TME (e.g., pH/hypoxia), wavelength engineering (e.g., NIR-II emission tuning), and immune-synergistic functionalization (e.g., light-controlled induction of ICD). These strategies underscore the unique advantages of AIEgens in spatiotemporally resolved diagnosis and therapy. They not only elucidate new mechanisms for precise "structure-function" correlations but also provide novel insights for the rational design of next-generation AIE photoactive materials. For easy reference, a selection of the representative molecules discussed herein is compiled in Table 1.

Despite the considerable promise of AIE materials in theranostics, their clinical translation continues to encounter multiple challenges, which align closely with the common limitations faced by photoactive agents in tumor therapy. The current bottlenecks are primarily reflected in the following aspects. In terms of biocompatibility and long-term toxicity, some organic AIE materials may induce immune responses or complement activation, necessitating surface modifications such as PEGylation or the incorporation of biocompatible moieties to reduce immunogenicity. Furthermore, the long-term accumulation of these materials in the reticuloendothelial system (e.g., liver and spleen) poses potential risks of chronic toxicity, underscoring the urgent need to develop metabolizable or degradable AIE systems (e.g., peptide- or carbohydrate-based AIEgens). Regarding targeting and penetration capabilities, AIE materials similarly suffer from insufficient tumor-specific accumulation and limited depth of penetration, impeded by biological barriers such as the BBB and the dense ECM. Concerning therapeutic mechanisms, a fundamental conflict exists between the efficacy and safety of phototherapies: PDT is often compromised by the hypoxic TME, while PTT carries a risk of thermal damage to surrounding healthy tissues. Additionally, the photostability and potential phototoxicity under prolonged illumination require systematic evaluation. On the industrialization front, challenges related to the scalable production and standardization of complex nanoarchitectures remain significant obstacles.

In recent years, AIE materials have made substantial strides in modulating the tumor immune microenvironment, offering novel strategies to transcend the limitations of mono-mechanistic therapies. For instance, AIE PSs can not only directly eliminate tumor cells during PDT but also induce ICD, leading to the release of DAMPs (e.g., HMGB1 and ATP), which facilitate DC maturation and antigen presentation. By loading M1-polarizing agents (e.g., TLR agonists) or engineering carriers responsive to pH/ROS, it is possible to reprogram TAMs from the pro-tumoral M2 phenotype to the antitumoral M1 phenotype, thereby enhancing antitumor immunity. Moreover, combining photothermal effects with immune checkpoint inhibitors (e.g., anti-PD-1 antibodies) has been shown to significantly increase tumor-infiltrating lymphocytes, converting immunologically "cold" tumors into "hot" ones.

Future development should focus on 3 core directions: first, establishing multimodal synergistic therapy platforms that integrate the phototherapeutic functions of AIE materials with immunotherapy, gene editing, and other advanced modalities; second, designing intelligent responsive systems based on AIE materials capable of sensing and reacting to multiple stimuli

(e.g., light, heat, pH, magnetic field) for precise monitoring and manipulation of the TME[176]; third, constructing an interdisciplinary clinical translation framework incorporating standardized toxicological evaluation, long-term animal studies, and AI-driven design optimization to accelerate the clinical application of AIE-based smart materials with multi-immunosignal sensing and responsive functionalities—ultimately enabling precise and controllable immuno-phototherapeutic synergy.

Acknowledgements

This study was financially supported by the Natural Science Foundation of Ningxia Province (Grant Nos. 2023AAC05027 and 2024AAC05045), the National Natural Science Foundation of China (Grant Nos. 22406096, 52303189, and U22A20144), and the Key Research and Development Program of Ningxia (Grant Nos. 2024SFZD004 and 2023BEG02023).

Conflicts of interests

The authors declare that they have no conflicts of interest.

Author Contributions

Chen Chen: Conceptualization, investigation, discussion, and writing original draft. Ping Wu and Feifan Zhao: Investigation, discussion, and writing original draft. Yuanyuan Han and Xiaoli Lu: Investigation and discussion. Huan Yu and Lingyan Huang: Discussion. Hao Wu: Discussion and supervision. Xiaoying Chen: Conceptualization, supervision, reviewing, and editing. Haijun Ma: Conceptualization, supervision, funding, review, and editing.

References

[1] Siegel RL, Kratzer TB, Giaquinto AN, et al. Cancer statistics, 2025. *CA Cancer J Clin*. 2025;75(1):10–45.
[2] May M. Targeted radiation adds precision to cancer therapy. *Nat Med*. 2025;31(3):702–703.
[3] Cai Y-Y, Chai T, Nguyen W, et al. Phototherapy in cancer treatment: strategies and challenges. *Signal Transduct Target Ther*. 2025;10(1):115.
[4] Sharma A, Yan J, Siwakoti P, et al. Morphology and temporal interactions of silica particles influence the chemotherapeutic cancer cell death. *Nano TransMed*. 2024;3:100053.
[5] Oh Y-J, Park SJ, Byun HK, et al. LLM-driven multimodal target volume contouring in radiation oncology. *Nat Commun*. 2024;15(1):9186.
[6] Yin X-R, Cheng Y-F, Feng Y, et al. Phototheranostics for multifunctional treatment of cancer with fluorescence imaging. *Adv Drug Deliv Rev*. 2022;189:114483.
[7] Ding Q, Guo A, Zhang S, et al. Phototheranostics: an advanced approach for precise diagnosis and treatment of gynecological inflammation and tumors. *Biomaterials*. 2025;316:123012.
[8] Repetowski P, Warszyńska M, Dąbrowski J-M. NIR-activated multifunctional agents for the combined application in cancer imaging and therapy. *Adv Colloid Interface Sci*. 2025;336:103356.
[9] Ding Q, Huang S, Zhang Z, et al. Integration of photodiagnosis and therapy guided by micro/nanorobots. *Adv Mater*. 2025;37(18):e2420359.
[10] Yang D-C, Wang S, Weng X-L, et al. Singlet oxygen-responsive polymeric nanomedicine for light-controlled drug release and image-guided photodynamic-chemo combination therapy. *ACS Appl Mater Interfaces*. 2021;13(29):33905–33914.
[11] Tan C, Li X, Li Z, et al. Near-infrared-responsive nanoplatforms integrating dye-sensitized upconversion and heavy-atom effect for enhanced photodynamic therapy efficacy. *Nano Today*. 2024;54:102089.
[12] Lee J, Lai S-J, Yang S-Y, et al. Bright and photostable yellow fluorescent proteins for extended imaging. *Nat Commun*. 2025;16(1):3241.
[13] Gao Z-Y, Zhang Y-F, Liu Q, et al. Mechanism and design of organic afterglow luminescent probes for cancer theranostics. *Med Mat*. 2024;1(1):27–39.
[14] Li G-Y, Wang C, Jin B-H, et al. Advances in smart nanotechnology-supported photodynamic therapy for cancer. *Cell Death Discov*. 2024;10(1):466.
[15] Zhou T-T, Hu R, Wang L-R, et al. An AIE-active conjugated polymer with high ROS-generation ability and biocompatibility for efficient photodynamic therapy of bacterial infections. *Angew Chem Int Ed Engl*. 2020;59(25):9952–9956.
[16] Cai X-L, Liu B. Aggregation-induced emission: recent advances in materials and biomedical applications. *Angew Chem Int Ed Engl*. 2020;59(25):9868–9886.
[17] Zhang G, Zhou D, Hu R, et al. Recent advances in aggregation-induced emission bioconjugates. *Bioconjug Chem*. 2025;36(4):609–626.
[18] Li W-X, Ai S-X, Zhu H-Y, et al. Activatable second-near-infrared-window multimodal luminogens with aggregation-induced-emission and aggregation-caused-quenching properties for step-imaging guided tumor therapy. *Nat Commun*. 2025;16(1):2471.
[19] Balachandran YL, Jiang X-Y. Aggregation-induced fluorogens in bio-detection, tumor imaging, and therapy: a review. *CCS Chem*. 2021;4(2):420–436.
[20] Ren K-Y, Zhang B-J, Guo J-C, et al. Aggregation-induced emission (AIE) for next-generation biosensing and imaging: a review. *Biosens Bioelectron*. 2025;271:117067.
[21] Meng Z-J, Xue H-Y, Wang T-T, et al. Aggregation-induced emission photosensitizer-based photodynamic therapy in cancer: from chemical to clinical. *J Nanobiotechnol*. 2022;20(1):344.
[22] Urazaliyeva A, Kanabekova P, Beisenbayev A, et al. All organic nanomedicine for PDT–PTT combination therapy of cancer cells in hypoxia. *Sci Rep*. 2024;14(1):17507.
[23] Wang J-H, Hou J-X, Lu H-J, et al. Engineering programmable nanobiomaterials (PNBMs) for cancer nanotherapy. *Med Mat*. 2025;2(1):1–16.
[24] Cen P-L, Huang J-N, Jin C-T, et al. Aggregation-induced emission luminogens for in vivo molecular imaging and theranostics in cancer. *Aggregate*. 2023;4(5):e352.
[25] Liu J-X, Chen W-T, Zheng C-Y, et al. Recent molecular design strategies for efficient photodynamic therapy and its synergistic therapy based on AIE photosensitizers. *Eur J Med Chem*. 2022;244:114843.
[26] Yu J, Wu J-Y, Huang J-S, et al. Hypoxia-tolerant polymeric photosensitizer prodrug for cancer photo-immunotherapy. *Nat Commun*. 2025;16(1):153.
[27] Li X, Lovell JF, Yoon JX, et al. Clinical development and potential of photothermal and photodynamic therapies for cancer. *Nat Rev Clin Oncol*. 2020;17(11):657–674.
[28] Ding Z-L, Gu Y-H, Zheng C, et al. Organic small molecule-based photothermal agents for cancer therapy: design strategies from single-molecule optimization to synergistic enhancement. *Coord Chem Rev*. 2022;464:214564.
[29] Lv Z, He S, Wang Y, et al. Noble metal nanomaterials for NIR-triggered photothermal therapy in cancer. *Adv Healthc Mater*. 2021;10(6):e2001806.
[30] Shen S, Qiu J, Huo D-Y, et al. Nanomaterial-enabled photothermal heating and its use for cancer therapy via localized hyperthermia. *Small*. 2024;20(7):e2305426.
[31] Yu L, Liu Z, Xu W, et al. Towards overcoming obstacles of type II photodynamic therapy: endogenous production of light, photosensitizer, and oxygen. *Acta Pharm Sin B*. 2024;14(3):1111–1131.
[32] Nestoros E, Sharma A, Kim E, et al. Smart molecular designs and applications of activatable organic photosensitizers. *Nat Rev Chem*. 2025;9(1):46–60.
[33] Riebe J, Bädorf B, Löffelsender S, et al. Molecular folding governs switchable singlet oxygen photoproduction in porphyrin-decorated bistable rotaxanes. *Commun Chem*. 2024;7(1):171.
[34] Wu R, Wang H-Z, Hai L, et al. A photosensitizer-loaded zinc oxide-polydopamine core-shell nanotherapeutic agent for photodynamic and photothermal synergistic therapy of cancer cells. *Chin Chem Lett*. 2020;31(1):189–192.
[35] Zhang Y-Y, Cheng Y-R, Yang F, et al. Near-infrared triggered Ti3C2/g-C3N4 heterostructure for mitochondria-targeting multimode photodynamic therapy combined photothermal therapy. *Nano Today*. 2020;34:100919.
[36] Cheng H-B, Cao X-Q, Zhang S-C, et al. BODIPY as a multifunctional theranostic reagent in biomedicine: self-assembly, properties, and applications. *Adv Mater*. 2023;35(18):2207546.

[37] Overchuk M, Weersink RA, Wilson BC, et al. Photodynamic and photothermal therapies: synergy opportunities for nanomedicine. *ACS Nano*. 2023;17(9):7979–8003.
[38] Shi J-Y, Fan Y-D, Zhang Q, et al. Harnessing photo-energy conversion in nanomaterials for precision theranostics. *Adv Mater*. 2025:2501623.
[39] Jeon J, You D-G, Um W, et al. Chemiluminescence resonance energy transfer–based nanoparticles for quantum yield–enhanced cancer phototheranostics. *Sci Adv*. 2020;6(21):eaaz8400.
[40] Ren Y, Yan Y, Qi H. Photothermal conversion and transfer in photothermal therapy: from macroscale to nanoscale. *Adv Colloid Interface Sci*. 2022;308:102753.
[41] Yang J, Ren B, Yin X-T, et al. Expanded ROS generation and hypoxia reversal: excipient-free self-assembled nanotheranostics for enhanced cancer photodynamic immunotherapy. *Adv Mater*. 2024;36(30):2402720.
[42] Lin R-F, Liu J-K, Xu W-L, et al. Type I photosensitization with strong hydroxyl radical generation in NIR dye boosted by vigorous intramolecular motions for synergistic therapy. *Adv Mater*. 2023;35(33):2303212.
[43] Zhao Y, Yuan B, Yan L, et al. In situ synthesis of Ru/TiO2–x@TiCN ternary heterojunctions for enhanced sonodynamic and nanocatalytic cancer therapy. *Adv Sci*. 2024;11(4):2307029.
[44] Zhang C-Y, Wang X, Du J-F, et al. Reactive oxygen species-regulating strategies based on nanomaterials for disease treatment. *Adv Sci (Weinh)*. 2021;8(3):2002797.
[45] Li J-Q, Zhuang Z-Y, Zhao Z-J, et al. Type I AIE photosensitizers: mechanism and application. *View*. 2022;3(2):20200121.
[46] Lapoot L, Jabeen S, O'Connor RM, et al. Photosensitized oxidative damage from a new perspective: the influence of before-light and after-light reaction conditions. *J Org Chem*. 2024;89(18):12873–12885.
[47] An X-Q, Yu W-F, Liu J-B, et al. Oxidative cell death in cancer: mechanisms and therapeutic opportunities. *Cell Death Dis*. 2024;15(8):556.
[48] Wang W-D, Sun Z-J. Evoking pyroptosis with nanomaterials for cancer immunotherapy: current boom and novel outlook. *Nano TransMed*. 2022;1(1):e9130001.
[49] Li B-H, Lin L. Internal light source for deep photodynamic therapy. *Light Sci Appl*. 2022;11(1):85.
[50] Shen Z-J, Ma Q-M, Zhou X-Y, et al. Strategies to improve photodynamic therapy efficacy by relieving the tumor hypoxia environment. *NPG Asia Mater*. 2021;13(1):39.
[51] Liu B-L, Zhou H-Y, Tan L-C, et al. Exploring treatment options in cancer: tumor treatment strategies. *Signal Transduct Target Ther*. 2024;9(1):175.
[52] Nomura S, Morimoto Y, Tsujimoto H, et al. Highly reliable, targeted photothermal cancer therapy combined with thermal dosimetry using a near-infrared absorbent. *Sci Rep*. 2020;10(1):9765.
[53] Chen G-C, Cao Y-H, Tang Y-X, et al. Advanced near-infrared light for monitoring and modulating the spatiotemporal dynamics of cell functions in living systems. *Adv Sci (Weinh)*. 2020;7(8):1903783.
[54] Bischof J, Fletcher G, Verkade P, et al. Multimodal bioimaging across disciplines and scales: challenges, opportunities and breaking down barriers. *NPJ Imaging*. 2024;2(1):5.
[55] Lin L-Y, Liu J-X, Pan Z-Y, et al. General post-regulation strategy of AIEgens' photophysical properties for intravital two-photon fluorescence imaging. *Adv Sci*. 2024;11(38):e2404792.
[56] Kim J, Lee S, Jeong Y, et al. Unlocking multimodal nonlinear microscopy for deep-tissue imaging under continuous-wave excitation with tunable upconverting nanoparticles. *Adv Mater*. 2025;37(19):2570137.
[57] Wang Z-J, Huang J-G, Huang J-S, et al. Chemiluminescence: from mechanism to applications in biological imaging and therapy. *Aggregate*. 2021;2(6):e140.
[58] Chen J-L, Liu T-Z, Gao J, et al. Variation in carbohydrates between cancer and normal cell membranes revealed by super-resolution fluorescence imaging. *Adv Sci*. 2016;3(12):1600270.
[59] Ouyang J, Xie A, Zhou J, et al. Minimally invasive nanomedicine: nan-otechnology in photo-/ultrasound-/radiation-/magnetism-mediated therapy and imaging. *Chem Soc Rev*. 2022;51(12):4996–5041.
[60] Zhang Z-J, Kang M-M, Tan H, et al. The fast-growing field of photo-driven theranostics based on aggregation-induced emission. *Chem Soc Rev*. 2022;51(6):1983–2030.
[61] Chu C-C, Yu J-W, Ren E, et al. Multimodal photoacoustic imaging-guided regression of corneal neovascularization: a non-invasive and safe strategy. *Adv Sci*. 2020;7(14):2000346.
[62] Yin J-Z, Lan L, Zhang Y, et al. Nanosecond-resolution photothermal dynamic imaging via MHZ digitization and match filtering. *Nat Commun*. 2021;12(1):7097.
[63] Liang Y-Z, Sun H-J, Cheng L-H, et al. High spatiotemporal resolution optoacoustic sensing with photothermally induced acoustic vibrations in optical fibres. *Nat Commun*. 2021;12(1):4139.
[64] Wen H-F, Zhang Z-J, Kang M-M, et al. One-for-all phototheranostics: single component AIE dots as multi-modality theranostic agent for fluorescence-photoacoustic imaging-guided synergistic cancer therapy. *Biomaterials*. 2021;274:120892.
[65] Doan V, Nguyen V, Mondal S, et al. Fluorescence/photoacoustic imaging-guided nanomaterials for highly efficient cancer theragnostic agent. *Sci Rep*. 2021;11(1):15943.
[66] Park J, Choi S, Knieling F, et al. Clinical translation of photoacoustic imaging. *Nat Rev Bioeng*. 2025;3(3):193–212.
[67] Zhang F, Cui J, Zhang Y, et al. Regulating aggregation-induced emission luminogen for multimodal imaging-navigated synergistic therapy involving anti-angiogenesis. *Adv Sci*. 2024;11(40):e2302713.
[68] Sun H-T, Zhang Q, Li J-C, et al. Near-infrared photoactivated nanomedicines for photothermal synergistic cancer therapy. *Nano Today*. 2021;37:101073.
[69] Zhang Z-Y, Du Y, Shi X-J, et al. NIR-II light in clinical oncology: opportunities and challenges. *Nat Rev Clin Oncol*. 2024;21(6):449–467.
[70] Pham T-C, Nguyen VN, Choi Y, et al. Recent strategies to develop innovative photosensitizers for enhanced photodynamic therapy. *Chem Rev*. 2021;121(21):13454–13619.
[71] Wang D-R, Wu X-L, Sun Y-L. Therapeutic targets and biomarkers of tumor immunotherapy: response versus non-response. *Signal Transduct Target Ther*. 2022;7(1):331.
[72] Deng X-Y, Shao Z-W, Zhao Y-L. Solutions to the drawbacks of photothermal and photodynamic cancer therapy. *Adv Sci (Weinh)*. 2021;8(3):2002504.
[73] Chen L, Hong W-Q, Ren W-Y, et al. Recent progress in targeted delivery vectors based on biomimetic nanoparticles. *Signal Transduct Target Ther*. 2021;6(1):225.
[74] Elhanani O, Ben-Uri R, Keren L. Spatial profiling technologies illuminate the tumor microenvironment. *Cancer Cell*. 2023;41(3):404–420.
[75] Bian W-Q, Wang Y, Pan Z-X, et al. Review of functionalized nanomaterials for photothermal therapy of cancers. *ACS Appl Nano Mater*. 2021;4(11):11353–11385.
[76] Zou J, Zhang Y, Pan Y, et al. Advancing nanotechnology for neoantigen-based cancer theranostics. *Chem Soc Rev*. 2024;53(7):3224–3252.
[77] Huang J-C, Zhang L-L, Wan D-L, et al. Extracellular matrix and its therapeutic potential for cancer treatment. *Signal Transduct Target Ther*. 2021;6(1):153.
[78] Chen Z, Han F-F, Du Y, et al. Hypoxic microenvironment in cancer: molecular mechanisms and therapeutic interventions. *Signal Transduct Target Ther*. 2023;8(1):70.
[79] Guo Y-D, Hu P, Shi J-L. Nanomedicine remodels tumor microenvironment for solid tumor immunotherapy. *J Am Chem Soc*. 2024;146(15):10217–10233.
[80] Shin J, Kang N, Kim B, et al. One-dimensional nanomaterials for cancer therapy and diagnosis. *Chem Soc Rev*. 2023;52(13):4488–4514.
[81] Laplane L, Maley CC. The evolutionary theory of cancer: challenges and potential solutions. *Nat Rev Cancer*. 2024;24(10):718–733.
[82] Xiang C-B, Liu Y, Ding Q-H, et al. Precise molecular engineering of multi-suborganelle targeted NIR type-I AIE photosensitizer and design of cell membrane-anchored anti-tumor pyroptosis vaccine. *Adv Funct Mater*. 2024;35(13):2417979.
[83] Zhuang J-B, Ma Z-D, Li N, et al. Molecular engineering of plasma membrane and mitochondria dual-targeted NIR-II AIE photosensitizer evoking synergetic pyroptosis and apoptosis. *Adv Mater*. 2023;36(5):2309488.
[84] Liang S-Y, Jiaerheng G, Huang C-J, et al. An endoplasmic reticulum-targeting and calcium metabolism-disrupting nanodrug enhances tumor photodynamic immunotherapy. *Adv Funct Mater*. 2025;35:2424108.
[85] Wang X, Qian J, Yang Z, et al. Photodynamic modulation of endoplasmic reticulum and mitochondria network boosted cancer immunotherapy. *Adv Mater*. 2024;36(4):e2310964.
[86] Hirabayashi K, Du H-W, Xu Y, et al. Dual-targeting CAR-T cells with optimal co-stimulation and metabolic fitness enhance antitumor activity and prevent escape in solid tumors. *Nat Cancer*. 2021;2(9):904–918.
[87] Wang X-Y, Chen Y, Li Y-F, et al. Advancing active compound discovery for novel drug targets: insights from AI-driven approaches. *Acta Pharmacol Sin*. 2025;1:1–12.
[88] Ma C-H, Gao L, Song K-W, et al. Targeted dual-responsive liposomes co-deliver jolkinolide B and Ce6 to synergistically enhance the

photodynamic/immunotherapy efficacy in gastric cancer through the PANoptosis pathway. *Adv Sci*. 2025;12(29):e02289.
[89] Stine ZE, Schug ZT, Salvino JMS, et al. Targeting cancer metabolism in the era of precision oncology. *Nat Rev Drug Discov*. 2022;21(2):141–162.
[90] Liu Z, Tang Z-M, Yin Y, et al. A microneedle patch delivers mitochondria- and lysosomes-dual targeting prodrug-like photosensitizers with regulated photoactivity for precise photodynamic therapy. *Adv Healthcare Mater*. 2025;14(9):2403954.
[91] Huang L, Qing D-Y, Zhao S-J, et al. Acceptor-donor-acceptor structured deep-red AIE photosensitizer: lysosome-specific targeting, in vivo long-term imaging, and effective photodynamic therapy. *Chem Eng J*. 2022;430:132638.
[92] Xiong T, Chen Y-C, Peng Q, et al. Lipid droplet targeting type I photosensitizer for ferroptosis via lipid peroxidation accumulation. *Adv Mater*. 2023;36(4):e2309711.
[93] Feng D-X, Jiao D, Xu H-D, et al. Supramolecular self-assembled endoplasmic reticulum-targeted peptide synergistically triggers type II ICD via cascade generation of endogenous ROS and RNS for cancer immunotherapy. *Adv Funct Mater*. 2025;35(37):2501271.
[94] You Y-J, Lai X, Pan Y, et al. Artificial intelligence in cancer target identification and drug discovery. *Signal Transduct Target Ther*. 2022;7(1):156.
[95] Li W, Zhou Z, Zhou X, et al. 3D biomimetic models to reconstitute tumor microenvironment in vitro: spheroids, organoids, and tumor-on-a-chip. *Adv Healthc Mater*. 2023;12(18):e2202609.
[96] Natesh NR, Varghese S. Advances and challenges in human 3D solid tumor models. *Adv Funct Mater*. 2025;35(20):2419912.
[97] Peng S-J, Xiao F-F, Chen M, et al. Tumor-microenvironment-responsive nanomedicine for enhanced cancer immunotherapy. *Adv Sci*. 2022;9(1):e2103836.
[98] Yuan X-L, Xiao Y, Yu D-H. Turn cold tumors hot by reprogramming the tumor microenvironment. *Nat Biotechnol*. 2025;43(4):466–470.
[99] Zhang L, Yu Y-W, Ding K-K, et al. Tumor microenvironment ameliorative and adaptive nanoparticles with photothermal-to-photodynamic switch for cancer phototherapy. *Biomaterials*. 2025;313:122771.
[100] Zhou W, Liu Y-C, Liu G-J, et al. Glycosylated AIE-active red light-triggered photocage with precisely tumor targeting capability for synergistic type I photodynamic therapy and CPT chemotherapy. *Angew Chem Int Ed*. 2024;64(1):e202413350.
[101] Shi Y-L, Yang W, Zhang H, et al. Near-infrared multiple-resonance polycyclic aromatic hydrocarbon as type I photosensitizer toward high-performance synergistic phototherapy. *Adv Funct Mater*. 2025;35(30):2423408.
[102] Hasegawa M, Maede K, Nishida M, et al. Abstract 1511: cancer adaptation to acidic tumor microenvironment. *Cancer Res*. 2025;85(8):1511–1511.
[103] Chen Q-W, Liu C-H, Fan J-X, et al. Self-mineralized photothermal bacteria hybridizing with mitochondria-targeted metal–organic frameworks for augmenting photothermal tumor therapy. *Adv Funct Mater*. 2020;30:1909806.
[104] Wang X, Wilhelm J, Li W, et al. Polycarbonate-based ultra-pH sensitive nanoparticles improve therapeutic window. *Nat Commun*. 2020;11(1):5828.
[105] Ding Q-H, Ding L, Xiang C-B, et al. pH-responsive AIE photosensitizers for enhanced antibacterial therapy. *Angew Chem Int Ed*. 2025;64(27):e202506505.
[106] Ferrentino N, Behroozi KT, Mehrtashfar S, et al. Dual-responsive nanoparticles for smart drug delivery: a NIR light-sensitive and redox-reactive PEG–PCL-based system. *Biomacromolecules*. 2024;25(12):7660–7673.
[107] Cheng G-H, Wang H-J, Zhang C-N, et al. Multifunctional nanophotosensitizer: a carrier-free aggregation-induced emission nanoparticle with efficient photosensitization and pH-responsibility. *Chem Eng J*. 2020;390:124447.
[108] Du J-Y, Su J-X, Xing Y, et al. Charge-reversal NaCl/G-quartets for aggregation-induced mitochondrial microRNA imaging and ion-interference therapy. *Anal Chem*. 2024;96(15):5922–5930.
[109] Xu Z-R, Li X, Yang Z-M, et al. An NIR-II two-photon excitable AIE photosensitizer for precise and efficient treatment of orthotopic small-size glioblastoma. *Adv Mater*. 2024;37(6):2413164.
[110] Sleeboom J, van Tienderen GS, Schenke-Layland K, et al. The extracellular matrix as hallmark of cancer and metastasis: from biomechanics to therapeutic targets. *Sci Transl Med*. 2024;16(728):eadg3840.
[111] He Z-J, Mao Y-X, Jian P. Tumor metabolism reprogramming provides novel targets for glioblastoma therapy. *J Ningxia Univ (Nat Sci Ed)*. 2024;45(2):186–195.
[112] Noorani I, Jorge DLR. Breaking barriers for glioblastoma with a path to enhanced drug delivery. *Nat Commun*. 2023;14(1):5909.
[113] Beygi M, Oroojalian F, Azizi-Arani S, et al. Multifunctional nanotheranostics for overcoming the blood–brain barrier. *Adv Funct Mater*. 2024;34(19):2310881.
[114] Wu D, Chen Q, Chen X-J, et al. The blood–brain barrier: structure, regulation and drug delivery. *Signal Transduct Target Ther*. 2023;8(1):217.
[115] Zeng Q, Li X-P, Li J-J, et al. Totally caged type I pro-photosensitizer for oxygen-independent synergistic phototherapy of hypoxic tumors. *Adv Sci*. 2024;11(31):e2400462.
[116] Zhang W-G, Kang M-M, Li X, et al. Fiber optic-mediated type I photodynamic therapy of brain glioblastoma based on an aggregation-induced emission photosensitizer. *Adv Mater*. 2024;36(47):2410142.
[117] Sarantopoulos A, Ene C, Aquilanti E. Therapeutic approaches to modulate the immune microenvironment in gliomas. *NPJ Precis Oncol*. 2024;8(1):241.
[118] Lee G-H, Lau VWH, Yang W, et al. Utilizing oxygen redox in layered cathode materials from multiscale perspective. *Adv Energy Mater*. 2021;11(27):2003227.
[119] Zheng M-J, Cao Y-F, Zhou Q-H, et al. Multifunctional zwitterionic N-oxide polymers to overcome cascade physiological barriers for efficient anticancer drug delivery. *Adv Healthc Mater*. 2025;14(7):2403852.
[120] Zhang P, Liu X, Guo P, et al. Effect of cyclic mechanical loading on immunoinflammatory microenvironment in biofabricating hydroxyapatite scaffold for bone regeneration. *Bioact Mater*. 2021;6(10):3097–3108.
[121] Pavuluri S, Sheth RA. Overcoming biophysical barriers with innovative therapeutic delivery approaches. *Cancer Gene Ther*. 2022;29(12):1847–1853.
[122] Sies H, Belousov V, Chandel NS, et al. Defining roles of specific reactive oxygen species (ROS) in cell biology and physiology. *Nat Rev Mol Cell Biol*. 2022;23(7):499–515.
[123] Lee D, Kwon S, Jang S, et al. Overcoming the obstacles of current photodynamic therapy in tumors using nanoparticles. *Bioact Mater*. 2022;8:20–34.
[124] Imberti C, Zhang P-Y, Huang H-Y, et al. New designs for phototherapeutic transition metal complexes. *Angew Chem Int Ed Engl*. 2020;59(1):61–73.
[125] Wang B-L, Hu S-Q, Teng Y, et al. Current advance of nanotechnology in diagnosis and treatment for malignant tumors. *Signal Transduct Target Ther*. 2024;9(1):200.
[126] Li Z, Tang B-Z, Wang D. Bioinspired AIE nanomedicine: a burgeoning technology for fluorescence bioimaging and phototheranostics. *Adv Mater*. 2024;36(32):e2406047.
[127] Zhang G-Q, Fu X-Y, Zhou D-M, et al. Smart aggregation-induced emission polymers: preparation, properties and bio-applications. *Smart Mol*. 2023;1(1):e20220008.
[128] Luo W-H, Wang G-J. Photo-responsive fluorescent materials with aggregation-induced emission characteristics. *Adv Opt Mater*. 2020;8(24):2001362.
[129] Sun J-M, Li H, Gu X-G, et al. Photoactivatable biomedical materials based on luminogens with aggregation-induced emission (AIE) characteristics. *Adv Healthc Mater*. 2021;10(24):2101177.
[130] Chen Y, Wang S-F, Zhang F. Near-infrared luminescence high-contrast in vivo biomedical imaging. *Nat Rev Bioeng*. 2023;1(1):60–78.
[131] Schmidt E-L, Ou Z-H, Ximendes E, et al. Near-infrared II fluorescence imaging. *Nat Rev Methods Primers*. 2024;4(1):23.
[132] Mao Z-Q, Rha H, Kim J, et al. THQ–xanthene: an emerging strategy to create next-generation NIR-I/II fluorophores. *Adv Sci*. 2023;10(18):2301177.
[133] Han Y-Y, Gao Q, Zhang X-H, et al. A high-performance organic fluorescent probe with aggregation-induced emission properties for long-term tumor monitoring. *Spectrochim Acta Part A*. 2024;319:124550.
[134] Ma H-J, Li R-X, Meng H, et al. A versatile theranostic nanoplatform with aggregation-induced emission properties: fluorescence monitoring, cellular organelle targeting, and image-guided photodynamic therapy. *Small*. 2023;19(21):2204778.
[135] Yan X-K, Sun Y, Tan Y-H, et al. A water-soluble aggregation-induced emission luminogen for NIR-I/NIR-II fluorescence imaging of breast cancer bone metastases. *Biosens Bioelectron*. 2025;268:116903.
[136] Barman D, Rajamalli P, Bidkar Anil P, et al. Modulation of donor in purely organic triplet harvesting AIE-TADF photosensitizer for image-guided photodynamic therapy. *Small*. 2025;21(7):2409533.
[137] Xu Y-Z, Dang D-F, Zhang N, et al. Aggregation-induced emission (AIE) in super-resolution imaging: cationic AIE luminogens (AIEgens)

for tunable organelle-specific imaging and dynamic tracking in nanometer scale. *ACS Nano*. 2022;16(4):5932–5942.
[138] He P, Tang H, Zheng Y, et al. Optical molecular imaging technology and its application in precise surgical navigation of liver cancer. *Theranostics*. 2025;15(3):1017–1034.
[139] Wang F-F, Zhong Y-T, Bruns O, et al. In vivo NIR-II fluorescence imaging for biology and medicine. *Nat Photonics*. 2024;18(6):535–547.
[140] Tan Y-H, Liu P-Y, Li D-X, et al. NIR-II aggregation-induced emission luminogens for tumor phototheranostics. *Biosensors*. 2022;12(1):46.
[141] Wang S-F, Li B-H, Zhang F. Molecular fluorophores for deep-tissue bioimaging. *ACS Cent Sci*. 2020;6(8):1302–1316.
[142] Jin Y-K, Xu K, Ren B-Y, et al. A spiro-based NIR-II photosensitizer with efficient ROS generation and thermal conversion performances for imaging-guided tumor theranostics. *Adv Healthc Mater*. 2025;14(7):2404783.
[143] Zheng P, Yan X-K, Zhu J, et al. Molecularly manipulating pyrazinoquinoxaline derivatives to construct NIR-II AIEgens for multimodal phototheranostics of breast cancer bone metastases. *Biomaterials*. 2025;317:123105.
[144] Zhang Z-J, Xu W-H, Kang M-M, et al. An all-round athlete on the track of phototheranostics: subtly regulating the balance between radiative and nonradiative decays for multimodal imaging-guided synergistic therapy. *Adv Mater*. 2020;32(36):2003210.
[145] You C-F, Zhu Y-Q, Zhu J, et al. Strength in numbers: a giant NIR-II AIEgen with one-for-all phototheranostic features for exceptional orthotopic bladder cancer treatment. *Angew Chem Int Ed*. 2024;64(6):e202417865.
[146] Song S-L, Zhao Y, Kang M-M, et al. An NIR-II excitable AIE small molecule with multimodal phototheranostic features for orthotopic breast cancer treatment. *Adv Mater*. 2024;36(14):e2309748.
[147] Zhang W-G, Kang M-M, Li X, et al. Interstitial optical fiber-mediated multimodal phototheranostics based on an aggregation-induced NIR-II emission luminogen for orthotopic breast cancer treatment. *Adv Mater*. 2024;36(38):2406474.
[148] Li D, Deng X-Q, Xu Z-R, et al. Molecular engineering of NIR-II AIE luminogen excited at 1700 nm for ultradeep intravital brain two-photon fluorescence imaging. *Adv Funct Mater*. 2023;33(46):2303967.
[149] Gong X-T, Dai X-Y, Cheng W, et al. Targeted high-resolution 3D imaging of tumor vasculatures at different stages using far-red AIE nanoparticles compatible with tissue clearing. *Adv Mater*. 2025;37(14):2501144.
[150] Yang Z-M, Zhang C, Zhang W-L, et al. Molecularly engineered high-performance AIE luminogen for NIR-III excitable deep-brain three-photon fluorescence imaging. *Chem Eng J*. 2024;496:153741.
[151] Qin W, Alifu N, Lam JWY, et al. Facile synthesis of efficient luminogens with AIE features for three-photon fluorescence imaging of the brain through the intact skull. *Adv Mater*. 2020;32(23):2000364.
[152] Yi M, Li T, Niu M, et al. Exploiting innate immunity for cancer immunotherapy. *Mol Cancer*. 2023;22(1):187.
[153] Sung C, An J, Lee S, et al. Integrative analysis of risk factors for immune-related adverse events of checkpoint blockade therapy in cancer. *Nat Cancer*. 2023;4(6):844–859.
[154] Lauss M, Phung B, Borch TH, et al. Molecular patterns of resistance to immune checkpoint blockade in melanoma. *Nat Commun*. 2024;15(1):3075.
[155] Park M, Lim J, Lee S, et al. Nanoparticle-mediated explosive anti-PD-L1 factory built in tumor for advanced immunotherapy. *Adv Mater*. 2025;37(7):2417735.
[156] Casagrande S, Sopetto GB, Bertalot G, et al. Immune-related adverse events due to cancer immunotherapy: immune mechanisms and clinical manifestations. *Cancers*. 2024;16(7):1440.
[157] Pantaleo G, Correia B, Fenwick C, et al. Antibodies to combat viral infections: development strategies and progress. *Nat Rev Drug Discov*. 2022;21(9):676–696.
[158] Wu S-Y, Wu F-G, Chen X-Y. Antibody-incorporated nanomedicines for cancer therapy. *Adv Mater*. 2022;34(24):2109210.
[159] Galluzzi L, Guilbaud E, Schmidt D, et al. Targeting immunogenic cell stress and death for cancer therapy. *Nat Rev Drug Discov*. 2024;23(6):445–460.
[160] Qi X-C, Li Q-L, Che X-Y, et al. Application of regulatory cell death in cancer: based on targeted therapy and immunotherapy. *Front Immunol*. 2022;13:837293.
[161] Fucikova J, Kepp O, Kasikova L, et al. Detection of immunogenic cell death and its relevance for cancer therapy. *Cell Death Dis*. 2020;11(11):1013.
[162] Del PA, Salvi V, Soriani A, et al. Dendritic cell subsets in cancer immunity and tumor antigen sensing. *Cell Mol Immunol*. 2023;20(5):432–447.
[163] Mishchenko T, Balalaeva I, Gorokhova A, et al. Which cell death modality wins the contest for photodynamic therapy of cancer? *Cell Death Dis*. 2022;13(5):455.
[164] Liu Z-Y, Zhang J-T, Liu H, et al. BSA-AIE nanoparticles with boosted ROS generation for immunogenic cell death immunotherapy of multiple myeloma. *Adv Mater*. 2022;35(7):2208692.
[165] Yang L, Huang J-C, Liao Y-A, et al. Strategically designed mitochondria-targeting AIEgens for effective eradication of primary and metastatic tumors via synergistic phototherapy and induced immunogenic cell death. *Adv Healthc Mater*. 2025;14(14):2500513.
[166] Sun Z-H, Liu J, Li Y-Y, et al. Aggregation-induced-emission photosensitizer-loaded nano-superartificial dendritic cells with directly presenting tumor antigens and reversed immunosuppression for photodynamically boosted immunotherapy. *Adv Mater*. 2022;35(3):2208555.
[167] Zhang G-Q, Chen X-M, Chen X, et al. Click-reaction-mediated chemotherapy and photothermal therapy synergistically inhibit breast cancer in mice. *ACS Nano*. 2023;17(15):14800–14813.
[168] Cui M-H, Tang D-S, Wang B, et al. Bioorthogonal guided activation of cGAS-STING by AIE photosensitizer nanoparticles for targeted tumor therapy and imaging. *Adv Mater*. 2023;35(52):2305668.
[169] Cao H-M, Gao H, Wang L-X, et al. Biosynthetic dendritic cell-exocytosed aggregation-induced emission nanoparticles for synergistic photodynamic immunotherapy. *ACS Nano*. 2022;16(9):13992–14006.
[170] Sun Z-H, Sun Z-K, Liu J, et al. Engineered extracellular vesicles expressing siglec-10 camouflaged aie photosensitizer to reprogram macrophages to active M1 phenotype and present tumor-associated antigens for photodynamic immunotherapy. *Small*. 2023;20(12):2307147.
[171] Wang Z-C, Tang Y-Q, Li Q. A self-assembling nanoplatform for pyroptosis and ferroptosis enhanced cancer photoimmunotherapy. *Light Sci Appl*. 2025;14(1):16.
[172] Li X, Ou X-W, Yang Z-M, et al. Win–win integration of genetically engineered cellular nanovesicles with high-absorbing multimodal phototheranostic molecules for boosted cancer photoimmunotherapy. *Adv Mater*. 2025;37(14):2416590.
[173] Wang B-G, Zhang G-Q, Chen Z-Z, et al. Lab-in-cell: a covalent photosensitizer reverses hypoxia and evokes ferroptosis and pyroptosis for enhanced anti-tumor immunity. *Adv Mater*. 2025;37(13):2415673.
[174] Ding D, Jiang X-Q. Advances in immunogenic cell death for cancer immunotherapy. *Small Methods*. 2023;7(5):2300354.
[175] Alzeibak R, Mishchenko TA, Shilyagina NY, et al. Targeting immunogenic cancer cell death by photodynamic therapy: past, present and future. *J Immunother Cancer*. 2021;9(1):e001926.
[176] Yuan X, Kang Y, Li R-Y, et al. Magnetically triggered thermoelectric heterojunctions with an efficient magnetic-thermo-electric energy cascade conversion for synergistic cancer therapy. *Nat Commun*. 2025;16(1):2369.

How to cite this article: Chen C, Wu P, Zhao F, Han Y, Lu X, Yu H, Huang L, Chen X, Ma H. Advances in organic photoactive materials with aggregation-induced emission characteristics for tumor theranostics. MedMat 2026;3(1):e00028. doi: 10.1097/mm9.0000000000000028